TREATMENT OF SOME HIGH AND LOW ENERGY HADRONIC TRANSITIONS IN THE FRAMEWORK OF BETHE-SALPETER DYNAMICAL PROGRAMME FOR A COMPOSITE HADRON

By

Elias Mengesha

SUBMITTED IN PARTIAL FULFILLMENT OF THE
REQUIREMENTS FOR THE DEGREE OF
DOCTOR OF PHILOSOPHY
AT
ADDIS ABABA UNIVERSITY
ADDIS ABABA, ETHIOPIA
FEB 2014

ADDIS ABABA UNIVERSITY
DEPARTMENT OF
PHYSICS

The undersigned hereby certify that they have read and recommend to the Faculty of Graduate Studies for acceptance a thesis entitled " **Treatment of some high and low energy hadronic transitions in the framework of Bethe-Salpeter dynamical programme for a composite hadron**" by **Elias Mengesha** in partial fulfillment of the requirements for the degree of **Doctor of Philosophy**.

Dated: Feb 2014

External Examiner: ______________________

Research Supervisor: ______________________
Dr. Shashank Bhatnagar

Examing Committee: ______________________

____

ADDIS ABABA UNIVERSITY

Date: **Feb 2014**

Author: **Elias Mengesha**

Title: **Treatment of some high and low energy hadronic transitions in the framework of Bethe-Salpeter dynamical programme for a composite hadron**

Department: **Physics**

Degree: **Ph.D.** Convocation: **July** Year: **2014**

Signature of Author

To my late mom.

Table of Contents

List of Figures

Abstract

In this thesis we employ Bethe Salpeter Equation(BSE) under Covariant Instantaneous Ansatz(CIA) to calculate: (A) The cross section of double Charmonium production from electron-positron annihilation at the CM energy $10.6GeV$ through the process $e^{+}+e^{-} \rightarrow J/\psi+\eta_c$, which has recently been observed at B factories and whose measurements were done by Babar and Belle groups. (B) The decay width for the radiative decay of equal mass vector mesons through the process $h \rightarrow h' + \gamma$(h=vector meson, h'=pseudoscalar meson and γ=the emitted photon.) (C) Decay width for strong decay of excited vector mesons through the process $h \rightarrow h' + h$"(h=excited vector meson, h'=vector meson and h"=pseudoscalar meson.) The calculated results are in reasonable agreement with data.

Acknowledgements

I am deeply indebted Dr.Shashank Bhatnagar, my advisor, for his useful suggestions, continuous support and friendly approach during this research. I am greatly acknowledge Haramaya University and Addis Ababa University for their continuous financial support and follow up during my study. I would also like to thank all members of the department of Physics, my family members and my friends for their continuous encouragement to finish my study.

Introduction

Quantum Chromodynamics(QCD) is regarded as correct theory for strong interactions. Quarks and gluons are the degrees of freedom of QCD. Investigation of bound states of quarks and gluons is one of the most effective methods to study the dynamics of its constituents. Understanding of hadronic properties is one of the most challenging tasks in strong interactions physics research. Although QCD is well established, there is still no consistent and straight forward way to describe low energy hadronic properties from QCD alone due to the fact that confinement potential can not yet be derived from QCD Lagrangian. Further due to large strength of running QCD coupling constant α_s at low and intermediate energies, the perturbation theory(which is quite successful in QED) will not work. Hence since the task of calculating hadron structures from QCD itself is very difficult(as can be also seen from various lattice QCD methods), one can rely on specific models to gain understanding of hadronic properties at low energies. This study can be most effectively be accomplished by applying a particular framework to a diverse range of phenomenon. The quark model for hadrons was first proposed by Gell-Mann and Zweig(1,2) as a realization of basic representation of SU(3) group. After this there has been a lot of work on various hadronic models that can calculate mass spectrum, decay widths, transition amplitudes of hadrons and hence explain properties such as confinement in

QCD. Some non-perturbative methods, such as lattice QCD calculation[3,4], nonrelativistic potential models[5] etc have been developed. However they have severe limitations. Nonrelativistic potential models are good for heavy quarkonia but they lack the Lorentz invariant dynamics needed for light quarkonia. Thus in potential models, the nonrelativistic character stands in the way of calculating anything meaningful beyond mass spectra and a few simple nonrelativistic transition amplitudes. The lattice gauge theory which is designed to solve strong interaction problem of QCD through discretization techniques tend to rapidly saturate the available computer size even in big institutions since results rely on numerical accuracy. Any realistic dynamical programme for a composite hadron must incorporate at minimum Lorentz and color gauge invariance for a consistent treatment of internal motion of constituents within a hadron. A natural dynamical link from low energies(mass spectra) and high energies(transition amplitudes) is most easily provided by a dynamical equation based approach if requirements of Lorentz and color gauge invariance are met. Standard dynamical equation for light quark physics is Bethe-Salpeter Equation(BSE). BSE is a conventional non perturbative approach in dealing with relativistic bound state problems in QCD. It is firmly established in the framework of quantum field theory and from the solutions we obtain useful information about the inner structure of hadrons which is crucial not only in low energy hadronic decays like $h \to h'\gamma$ and $h \to h'h$"(studied in the latter part of this thesis) but also high energy hadronic scattering and production processes like $e^+ + e^- \to J/\psi + \eta_c$(studied in the first part of this thesis). Despite its drawback of having to input model dependent kernel, these studies have become an interesting topic in recent years since calculations have shown that BSE framework using phenomenological potentials can give satisfactory results as more and more data is being accumulated. We get useful insight about the treatment of various processes using BSE due to the unambiguous definition of the 4 dimensional BS wave function which provides an effective coupling vertex(hadron-quark vertex) of hadron with all its constituents(quarks). Thus hadron-quark vertex is considered to sum up all the nonperturbative QCD effects in the hadron. However the complexities of BSE have tended to encourage different version of this equation mostly based on 3 dimensional reduction techniques such as the Covariant Instantaneous Ansatz(CIA) which we employ in our work. The purpose of this work is to test Bethe-Salpeter Equation(BSE) under CIA and to provide justification to the theory proposed about the substructure of hadrons. The main focus of this work is to calculate the cross section and the decay widths of some hadronic processes at low and high energies. This thesis is organized as follows: Chapter 1 deals with a brief review of the SU(3) gauge theory(QCD). Chapter 2 deals with Bethe-Salpeter Equation. Chapter 3 deals with the calculation of cross section of high energy production process: $e^+ + e^- \rightarrow J/\psi + \eta_c$ at center of mass energy 10.6GeV which is recently observed at B-factories and whose measurements have been performed by Babar and Belle groups. Chapter 4 deals with some low energy hadronic decays proceeding through triangle quark loop diagrams such as (i) radiative decays of ground state vector mesons through the process $h \rightarrow h'\gamma$ and the strong decays of excited vector mesons through the process $h \rightarrow h'h''$. We have proposed a way of handling complexities which appear in triangle loop diagrams in BSE under CIA. Chapter 5 is devoted to summary and conclusion.

Chapter 1

Quantum Chromodynamics(QCD)

1.1 Introduction

Quantum chromodynamics (QCD) is considered as the gauge theory of strong interactions. For some earlier classic reference see reference[6,7]. The physical degrees of freedom are quarks and gluons. Gluons are the quanta of gauge fields which are in some ways analogous to photons in QED. The crucial difference is that gluons couple directly to each other, whereas photons do not. A consequence of the self-coupling of gluons is that the force between quarks does not vanish at large distances but becomes a constant $F_{QCD} \approx 800 MeV fm^{-1} \approx 15,000 N$[8]. This is in contrast to the coulomb force between two charges which goes as $\sim \frac{1}{r^2}$ and hence vanishes at large distances. It would, thus, require a vast amount energy to separate quarks out to a macroscopic distance. Indeed, long before the separation becomes large enough to measure, the energy stored in the gluon field "sparks" into quark-antiquark pairs. This phenomenon of QCD explains why freely propagating quarks are not observed in nature, and it is called confinement.

QCD is a non Abelian SU(3) gauge theory in contrast to QED which is an Abelian

U(1) gauge theory. The most widely used theoretical tool for quantum field theories is relativistic perturbation theory, as developed for quantum electrodynamics (QED) by Feynman, Schwinger, Tomonaga and others sixty years ago [9]. Perturbation theory provides the key connection between the mathematical theory with experiments in QED and the Glashow-Weinberg-Salam theory merging QED with the weak nuclear force [10].

A textbook example of perturbative quantum field theory is to calculate how virtual pairs induce a distance dependence on the coupling in quantum gauge theories. In QED, one considers the fine structure constant,

$$\alpha = \frac{e^2}{4\pi\hbar c}, \tag{1.1.1}$$

where -e is the charge of the electron. In QCD, one has the strong coupling α_s , related to the gauge coupling g by analogy with Eq.(1.1.1). When virtual pairs are taken into account, α and α_s are not constant but depend on distance; they are said to "run." The running, depicted in figure 1[8], is completely different in the two theories. In QED α becomes constant at distances $r > \frac{\hbar}{m_e c}$ (the electron's Compton wavelength), but at short distances it grows. In QCD α_s grows at long distance; perturbative running no longer makes sense once r is in the confining regime. At short distances-or, equivalently, high energies-the QCD coupling is small enough that perturbation theory can again be used. For example, the cross section for an electron- positron pair to annihilate and produce a quark-antiquark pair can be reliably computed as a power series in α_s. The quark and antiquark each fragment into a jet of hadrons-mostly pions, but some protons and neutrons, too-and general properties such as the energy flow and angular distributions of these jets can be traced back to the quark and antiquark. In this way, the experiments can measure quark properties, and these are found to agree with theoretical calculations [11]. In this thesis we will use natural units, i.e.; $\hbar = c = 1, e > 0$, and $\alpha = \frac{e^2}{4\pi} \approx \frac{1}{137}$.

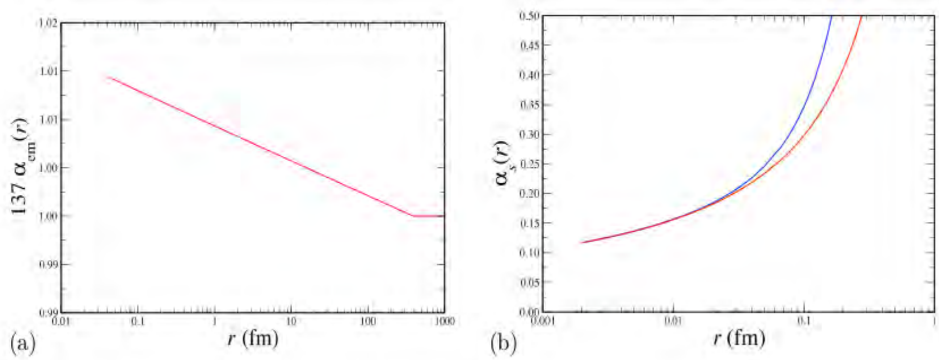

Figure 1.1: Running of (a) the QED and (b) the QCD coupling with distance. For QCD the lower curve shows the perturbative result, and the higher shows the effect of confining forces.

1.2 QCD Lagrangian and it symmetries

The gauge principle has proven to be a tremendously successful method in elementary particle physics to generate interactions between matter fields through the exchange of massless gauge bosons (for details see reference[7]). The best known example is, of course, quantum electrodynamics(QED) which is obtained from promoting the global U(1) symmetry of the Lagrangian describing a free electron,

$$\Psi \to e^{(i\Theta)}\Psi : \pounds_{free} = -\overline{\Psi}(\gamma_\mu \partial_\mu + m)\Psi \to \pounds_{free}, \tag{1.2.2}$$

to a local symmetry, where Ψ is the electron field and $\overline{\Psi} = \Psi^\dagger \gamma_4$. In this process the parameter $0 \leq \Theta \leq 2\pi$ describing an element of U(1) is allowed to vary smoothly in space time, $\Theta \to \Theta(x)$, which is referred to as gauging the U(1) group. To keep the invariance of the Lagrangian under local transformations one introduces a four potential $A_\mu \longrightarrow A_\mu - \frac{\partial_\mu \Theta}{e}$. This method is referred to as gauging the Lagrangian with respect to U(1):

$$\pounds_{QED} = -\overline{\Psi}(\gamma_\mu(\partial_\mu - ieA_\mu) + m)\Psi - \frac{1}{4}F_{\mu\nu}F_{\mu\nu}, \tag{1.2.3}$$

where $F_{\mu\nu} = \partial_\mu A_\nu - \partial_\nu A_\mu$. The covariant derivative of Ψ,

$$D_\mu \Psi = (\partial_\mu - ieA_\mu)\Psi, \tag{1.2.4}$$

is defined such that under a so called gauge transformation of the second kind

$$\Psi \rightarrow e^{[-i\Theta(x)]}\Psi, \tag{1.2.5}$$

$$A_\mu \rightarrow A_\mu - \frac{\partial_\mu \Theta(x)}{e}, \tag{1.2.6}$$

it transforms in the same way as Ψ itself:

$$D_\mu \Psi \rightarrow e^{[-i\Theta(x)]} D_\mu \Psi. \tag{1.2.7}$$

In Eq.(1.2.3), the term containing the squared field strength makes the gauge potential a dynamical degree of freedom as opposed to a pure external field. A mass term $\frac{M^2 A^2}{2}$ is not included since it would violate gauge invariance and thus the gauge principle requires massless gauge bosons.

In the same analogy, the QCD Lagrangian obtained from the gauge principle reads

$$\pounds_{QCD} = -\sum_{f=u,d,s,c,b,t} \overline{q}_f(\not{D} + m_f)q_f - \frac{1}{4}G_{\mu\nu,a}G_{\mu\nu,a}, \tag{1.2.8}$$

where q_f is the quark field and $\overline{q}_f = q^\dagger \gamma_4$. For each quark flavor f the quark field q_f consists of a color triplet(subscripts r, g, and b standing for "red," green," and "blue"),

$$q_f = \begin{pmatrix} q_{f,r} \\ q_{f,g} \\ q_{f,b} \end{pmatrix} \tag{1.2.9}$$

which transforms under a gauge transformation $g(x)$ described by the set of parameters $\Theta(x) = [\Theta_1(x), ..., \Theta_8(x)$ according to

$$q_f \to q'_f = e^{[-i\sum_{a=1}^{8}\Theta_a(x)\frac{\lambda_a^c}{2}]}q_f = U[g(x)]q_f. \tag{1.2.10}$$

c indicating the action in color space and λ_a being the generators of the gauge group which satisfies $[\frac{\lambda_a}{2}, \frac{\lambda_b}{2}] = if_{abc}\frac{\lambda_c}{2}$ where f_{abc} are the structure constants of SU(3) and antisymmetric. Because SU(3) is an eight parameter group, the covariant derivative of Eq.(1.2.8) contains eight independent gauge potentials A_μ, a,

$$D_\mu \begin{pmatrix} q_{f,r} \\ q_{f,g} \\ q_{f,b} \end{pmatrix} = \partial_\mu \begin{pmatrix} q_{f,r} \\ q_{f,g} \\ q_{f,b} \end{pmatrix} - ig\sum_{a=1}^{8}\frac{\lambda_a^c}{2}A_{\mu,a} \begin{pmatrix} q_{f,r} \\ q_{f,g} \\ q_{f,b} \end{pmatrix}. \tag{1.2.11}$$

We note that the interaction between quarks and gluons is independent of the quark flavors and we define g as the strong coupling constant. Demanding gauge invariance of $\pounds_{QCD}$ imposes the following transformation property of the gauge fields

$$\frac{\lambda_a^c}{2}A_{\mu,a}(x) \to U[g(x)]\frac{\lambda_a^c}{2}A_{\mu,a}(x)U^\dagger[g(x)] - \frac{i}{g}\partial_\mu U[g(x)]U^\dagger[g(x)]. \tag{1.2.12}$$

Again, with this requirement the covariant derivative $D_\mu q_f$ transforms as q_f, i.e., $D_\mu q \to D'_\mu q' = U(g)D_\mu q$.

So far we have considered the matter field part of $\pounds_{QCD}$ including its interaction with the gauge fields. Eq.(1.2.8) also contains the generalization of the field strength tensor to the non Abelian case,

$$G_{\mu\nu,a} = \partial_\mu A_{\nu,a} - \partial_\nu A_{\mu,a} + gf_{abc}A_{\mu,b}A_{\nu,c}. \tag{1.2.13}$$

Given Eq.(1.2.12) the field strength tensor transforms under SU(3) as

$$G_{\mu\nu} = \frac{\lambda_a^c}{2} G_{\mu\nu,a} \rightarrow U[g(x)] G_{\mu\nu} U^{\dagger}[g(x)]. \tag{1.2.14}$$

In contradiction to the Abelian case of QED, the squared field strength tensor gives rise to gauge field self interactions involving vertices with three and four gauge fields of strength g and g^2, respectively. Such interaction terms are characteristic of non Abelian gauge theories and make them much more complicated than Abelian theories. Substituting Eq.(1.2.11) and Eq.(1.2.13) into Eq.(1.2.8), the full Lagrangian is given by

$$\begin{aligned}
\pounds_{QCD} = \quad & -\sum_f \overline{q}_f (\gamma_\mu \partial_\mu + m_f) q_f \\
& + ig \sum_f \overline{q}_f A_{\mu,a} \frac{\lambda_a}{2} q_f \\
& - \frac{1}{4} (\partial_\mu A_{\nu,a} - \partial_\nu A_{\mu,a})^2 \\
& - \frac{g}{4} A_{\mu,b} A_{\nu,c} f_{abc} (\partial_\mu A_{\nu,a} - \partial_\nu A_{\mu,a}) \\
& - \frac{g}{4} f_{ade} (\partial_\mu A_{\nu,a} - \partial_\nu A_{\mu,a}) A_{\mu,d} A_{\nu,e} \\
& - \frac{g^2}{4} f_{abc} f_{ade} A_{\mu,b} A_{\nu,c} A_{\mu,d} A_{\nu,e}.
\end{aligned} \tag{1.2.15}$$

The first term in Eq. (1.2.15) is Lagrangian for the matter fields and using the Feynman rules, it is represented by the diagram shown in Fig.(1.2).

Figure 1.2: Diagram for the interaction of matter

Similarly the second term(interaction Lagrangian) is represented by the diagram shown in Fig.(1.3).

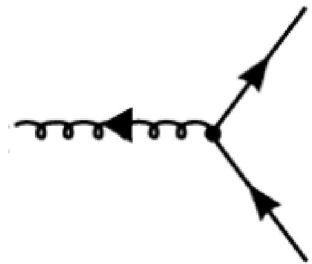

Figure 1.3: Diagram for the interaction part

The third term (the gluon kinetic term) is represented by the diagram shown in Fig.(1.4).

Figure 1.4: Feynman diagram for the kinetic part

The fourth and fifth terms(self interaction among three gluons) are represented by the diagram shown in Fig.(1.5).

Figure 1.5: Self interaction among three gluons.

Finally the last term (self interaction among four gluons) is represented by the diagram shown in Fig.(1.6).

Figure 1.6: self interaction among four gluons.

1.3 Higher orders, divergences and renormalization

If we wish to calculate the amplitude (or cross section) for a particular process in lowest order, we must evaluate the amplitudes contributing from all possible lowest order graphs using Feynman rules. Lowest order graphs are called Born diagrams and involve only tree diagrams; that is, diagrams which can be constructed without closed loop. On the other hand, if we wish to calculate the cross section for a particular physical process to order n in the perturbation series expansion, then all possible diagrams which can give a contribution to this order must be evaluated. Now these diagrams contain graphs containing loops. Graphs containing loops lead to divergent integrals in the evaluation of the cross sections and thus present an additional theoretical problem in QED and QCD. In order to get a finite value from the divergent integral, the integral must first be regularized. Next, the potentially divergent parts are renormalized in terms of physically measurable quantities (mass, charge). The final result should not depend on the regularization methods and also it should be gauge invariant result. Dimensional regularization is one of the powerful methods of regularization. It is widely employed in QED and QCD. In the next section we will employ dimensional regularization to calculate the running coupling constant of QCD.

1.4 Renormalized coupling constant of QCD

For QED, the renormalized coupling constant as a function of momentum Q^2 is given by

$$\alpha(Q^2) = \frac{\alpha(0)}{1 - \frac{\alpha(0)}{3\pi} Log(\frac{Q^2}{m^2})}, \frac{Q^2}{m^2} \gg 1,$$

where $\alpha(0) = \frac{1}{137}$ is the fine structure constant. The variation of $\alpha(Q^2)$ is small as Q^2 increases. Thus, perturbation theory is very well applicable for any accessible energy regimes.

We shall now use dimensional regularization[12] to calculate the renormalized QCD coupling constant to lowest order. The divergent graphs contributing to the renormalization of g belong to three classes, shown in Figs. 1.7, 1.8, and 1.9. Let us work them out one by one.

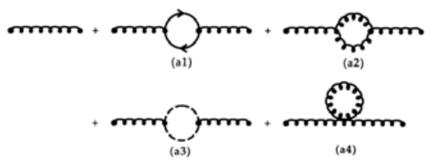

Figure 1.7: The vacuum polarization of QCD.

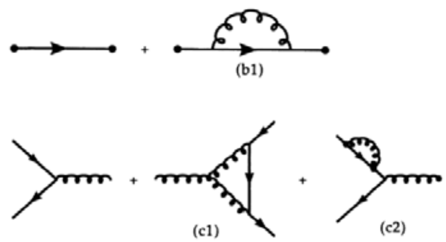

Figure 1.8: The self energy graph of QCD.

Graph (al). We start with vacuum polarization, in particular with the fermion graph (al) in Fig. 1.7. This graph is depicted in greater detail in Fig. 1.10. One may wonder why the quantum numbers of the outgoing gluon k', a', μ' are not identical with those of the ingoing gluon. Of course, this is the most general case. It will turn out that indeed a = a' and $k = k'$ (momentum conservation), but $\mu' \neq \mu$.

Using the QCD Feynman rules it is easy to write down the polarization tensor:

$$\Pi^{aa'(al)}_{\mu\mu'}(K) = -\sum_{1}^{N_f} g^2 \int \frac{d^4q}{(2\pi)^4} Tr[\frac{(-i\gamma.(K+q)+m)\gamma_\mu(-i\gamma.q+m)\gamma_{\mu'}}{[(K+q)^2+m^2+i\eta][q^2+m^2+i\eta]} Tr(\frac{\lambda_a\lambda_{a'}}{4}). \tag{1.4.16}$$

N_f is number of quarks and using dimensional regularization [12] $\Pi_{\mu\mu'}(K)$ is given by

$$\Pi^{aa'(al)}_{\mu\mu'}(K) = ig^2\frac{n_f}{16\pi^2}\frac{2}{3}(\frac{1}{\epsilon} - LogK^2 + const)(\delta_{\mu\mu'}K^2 - K_\mu K_{\mu'}), \tag{1.4.17}$$

where ϵ is a very small number and closer to zero and when it is zero the above equation will be infinity but in the renormalization it will be subtracted out and absorbed in the coupling constant. For details see reference [12].

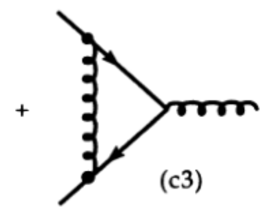

Figure 1.9: The vertex correction graph of QCD.

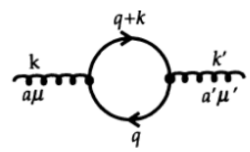

Figure 1.10: The variables chosen for the quark loop contribution to vacuum polarization.

Graph (a2). Next we calculate the gluon loop with two 3-gluon vertices as shown in figure below.

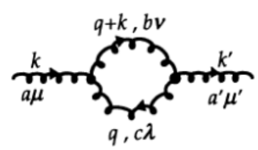

Figure 1.11: The chosen variables from the first gluon loop contribution to vacuum polarization.

Using Feynman rules, the gluon loop tensor is given by:

$$\begin{aligned}\Pi^{aa'(a2)}_{\mu\mu'}(K) = \quad & \frac{g^2}{2}\int\frac{d^4q}{(2\pi)^4}f_{abc}[\delta_{\mu\lambda}(K-q)_\nu+\delta_{\nu\mu}(-q-2K)_\lambda+\delta_{\lambda\nu}(2q+K)_\mu] \\ & x f_{a'bc}[\delta_{\mu'\lambda}(-K+q)_\nu+\delta_{\nu\mu'}(q+2K)_\lambda+\delta_{\nu\lambda}(-2q-K)_\mu] \\ & x\frac{1}{[(q+K)^2+i\eta]}\frac{1}{[q^2+i\eta]}. \end{aligned} \tag{1.4.18}$$

From the above integral, one can obtain

$$\Pi^{aa'(a2)}_{\mu\mu'}(K) = 3i\frac{g^2\delta_{aa'}}{16\pi^2}\frac{1}{12}(\frac{1}{\epsilon} - LogK^2 + const)(-19\delta_{\mu\mu'}K^2 + 22K_\mu K_{\mu'}). \quad (1.4.19)$$

This expression is not gauge invariant($K_\mu \Pi^{aa'}_{\mu\mu'} \neq 0$). Gauge invariance is only restored by including the ghost terms. More precisely the ghost fields are constructed such that they cancel the contribution from the unphysical degrees of freedom of the gluon field. These unphysical degrees of freedom violate the gauge symmetry.

Graph (a3). To see how this happens we next calculate the ghost contribution. The details of graph(a3) is shown in figure below.

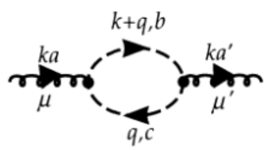

Figure 1.12: The chosen variables for the ghost loop contribution to vacuum polarization, b and c describe the color of the ghosts .

Using Feynman rules, the ghost loop tensor is given by:

$$\Pi^{aa'(a3)}_{\mu\mu'}(K) = -g^2 f_{abc} f_{a'bc} \int \frac{d^4q}{(2\pi)^4} \frac{q_{\mu'}(K+q)_\mu}{[(q+K)^2 + i\eta][q^2 + i\eta]}. \quad (1.4.20)$$

Using the technique used for quark and gluon loops, we can obtain

$$\Pi^{aa'(a3)}_{\mu\mu'}(K) = 3i\frac{g^2\delta_{aa'}}{16\pi^2}\frac{1}{12}(\frac{1}{\epsilon} - LogK^2 + const)(-\delta_{\mu\mu'}K^2 - 2K_\mu K_{\mu'}). \quad (1.4.21)$$

Summing over the contributions from the gluon loop(Fig.1.11) and ghost loop(Fig.1.12) we get

$$\Pi^{aa'(a2)}_{\mu\mu'}(K) + \Pi^{aa'(a3)}_{\mu\mu'}(K) = i\frac{3g^2}{16\pi^2}\delta_{aa'}(\frac{1}{\epsilon} - Logk^2 + constant)\frac{20}{12}(K_\mu K_{\mu'} - \delta_{\mu\mu'}K^2). \quad (1.4.22)$$

Thus we see that

$$K_\mu(\Pi^{aa'(a2)}_{\mu\mu'}(K) + \Pi^{aa'(a3)}_{\mu\mu'}(K)) = 0, \tag{1.4.23}$$

which is gauge invariant.

Graph (a4). The contribution for graph(a4) is proportional to $\int \frac{d^4q}{q^2} = 0$.

The total contribution from Fig.(1.7) is given by

$$(K_\mu K_{\mu'} - \delta_{\mu\mu'}K^2)\frac{g^2}{16\pi^2}(\frac{1}{\epsilon} - LogK^2 + const)(\frac{20}{12}c_2 - \frac{2}{3}n_f), \tag{1.4.24}$$

where c_2 is color factor(=3) and n_f is number of quarks.

Graph (bl). Next we calculate the self-energy graph. To simplify let us ignore the mass of the quark. The details of the self energy graph is shown in figure below.

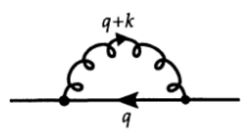

Figure 1.13: The chosen variables for the self-energy graph.

The contribution from the self energy graph is given by

$$\sum^b(K) = g^2 \int \frac{d^4q}{(2\pi)^4} \frac{\gamma_\mu \not{q} \gamma_\mu \frac{\lambda_a}{2}\lambda_a}{2} \frac{1}{[(q+K)^2 + i\eta]} \frac{1}{[q^2 + i\eta]}. \tag{1.4.25}$$

Using the same methods in the above cases, one can obtain

$$\sum^b(K) = \frac{4}{3}g^2 \frac{i}{16\pi^2}(\frac{1}{\epsilon} - LogK^2 + const)\not{K}. \tag{1.4.26}$$

Graph (cl). The vertex corrections.

The details of the vertex correction graph is shown in figure below. Let us ignore the mass of the quark.

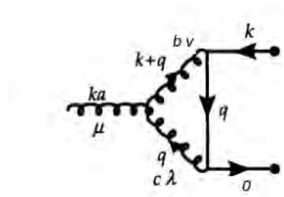

Figure 1.14: The chosen variables for the vertex correction graph.

The contribution from Graph(c1) is given by

$$\Gamma_{\mu^{a(c1)}} = -ig^3 \int \frac{d^4q}{(2\pi)^4} f_{abc}[\delta_{\mu\lambda}(K-q)_\nu + \delta_{\nu\mu}(-q-2K)_\lambda + \delta_{\lambda\nu}(2q+K)_\mu]\frac{\lambda_b\lambda_c}{4}$$
$$\frac{\gamma_\nu \not{q} \gamma_\lambda}{[(q+K)^2+i\eta]}\frac{1}{[q^2+i\eta]^2}. \qquad (1.4.27)$$

Using dimensional regularization we get

$$\Gamma_{\mu^{a(c1)}} = ic_2\frac{\lambda_a}{2}3g^3\frac{\gamma_\mu}{32\pi^2}(\frac{1}{\epsilon} - LogK^2 + const). \qquad (1.4.28)$$

Graph (c2). Adopting again the same kinematics as for the calculation of (cl), the contribution from the second vertex graph Fig. (1.15) is

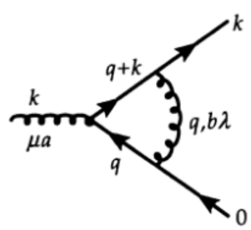

Figure 1.15: The chosen variables for the second vertex correction graph.

$$\Gamma_\mu^{a(c2)} = g^3 \int \frac{d^4q}{(2\pi)^4}\frac{\lambda_b}{2}\gamma_\lambda\frac{\lambda_a}{2}(\not{q}+\not{K})\gamma_\mu\not{q}\frac{\lambda_b}{2}\gamma_\lambda\frac{1}{[(q+K)^2+i\eta][q^2+i\eta]^2}. \qquad (1.4.29)$$

Using dimensional regularization we obtain,

$$\Gamma_\mu^{a(c2)} = ig^3(\frac{4}{3} - \frac{c_2}{2})\frac{\lambda_a}{2}\frac{\gamma_\mu}{16\pi^2}(\frac{1}{\epsilon} - LogK^2 + const). \qquad (1.4.30)$$

Summing one loop contributions from Fig.(1.14) and Fig.(1.15) to vertex correction, taking into consideration the exchange diagrams as well, we obtain

$$\Gamma_\mu(K) = 2(\Gamma_\mu^{a(c1)} + \Gamma_\mu^{a(c2)}), \tag{1.4.31}$$

which is given by

$$\Gamma_\mu(K) = i\frac{g^3}{16\pi^2}\frac{\lambda_a}{2}\gamma_\mu(c_F + c_A)(\frac{1}{\epsilon} - LogK^2 + const), \tag{1.4.32}$$

where color factor $c_F = \frac{N^2-1}{2N}, c_A = N$, and N is number of colors. We have already seen that the total contribution from sum of one loop corrections to gluon self energy in Fig.(1.7) as

$$\Pi_{\mu\mu'}(K) = i\frac{g^2}{24\pi^2}N_f(\frac{1}{\epsilon} - LogK^2 + const). \tag{1.4.33}$$

Now the total vertex modification with contributions from tree level to one loop level can be shown diagrammatically as in Fig.(1.16). The contribution from Fig.(1.16)

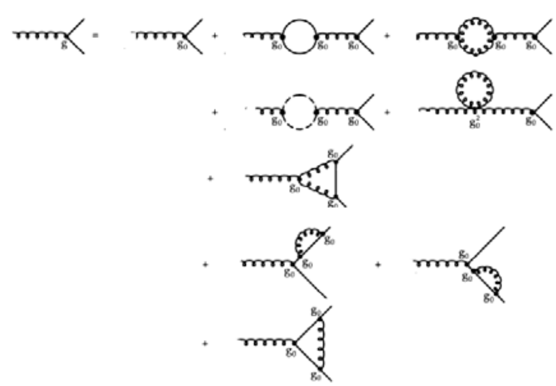

Figure 1.16: Higher order corrections diagrams from tree level to one loop level .

can be expressed as

$$i\frac{\delta_{\mu\mu'}}{K^2}\Gamma[\overline{u}_1(ig\frac{\lambda_a}{2}\gamma_\mu)u_1] = \overline{u}_1\Gamma_\mu^{total}u_1, \tag{1.4.34}$$

where $\Gamma = g_0 + \frac{g^3}{16\pi^2}(\frac{11}{3}c_A - \frac{2}{3}N_F)(\frac{1}{\epsilon} - LogK^2 + const)$, c_A is number of colors and N_F is number of flavors. The renormalized coupling constant is obtained from the above equation by subtracting the value of the correction at some renormalization energy scale M^2 as,

$$g_R = g_0 - \frac{g^3}{16\pi^2}(\frac{11}{6}c_A - \frac{1}{3}N_F)(\frac{1}{\epsilon} - LogK^2 - \frac{1}{\epsilon} + LogM^2), \tag{1.4.35}$$

which can expressed as

$$g_R = g_0 + \frac{g^3}{16\pi^2}(\frac{11}{6}c_A - \frac{1}{3}N_F)Log\frac{K^2}{M^2}. \tag{1.4.36}$$

After a series of steps it can be shown that the QCD running coupling constant[12] can be expressed as,

$$\alpha_s(Q^2) = \frac{12\pi}{(33 - 2N_F)Log[\frac{Q^2}{\Lambda^2_{QCD}}]}, \tag{1.4.37}$$

where $Q^2 = K^2$ and Λ_{QCD} is taken as the energy scale where the effective coupling becomes large at sufficiently low Q^2. At $Q^2 \gg \Lambda^2_{QCD}$, $\alpha_s(Q^2)$ is small and a perturbative description in terms of quarks and gluons interacting weakly makes sense. For $Q^2 \approx \Lambda^2_{QCD}$, the perturbative expansion will not make sense since quarks and gluons are strongly bound into hadrons. Thus we can regard Λ_{QCD} as s boundary between a world of free quarks and gluons and a world of mesons, baryons, etc. The value of Λ_{QCD} is not predicted by theory but is free parameter to be determined by experiment. One expects Λ_{QCD} to be of the order of a typical hadronic mass. Most works take Λ_{QCD} value to be in the range of 0.1GeV to 0.5GeV. For $K = X\Lambda_{QCD}$, where x is any positive number and $N_F = 6$, the variation of α_s as function of momentum is shown in figure below. As we see from Fig.(1.1) and Fig.(1.17), α_s increases as the momentum transfer Q^2 is smaller (or as separation(r) increases) and vice versa. From

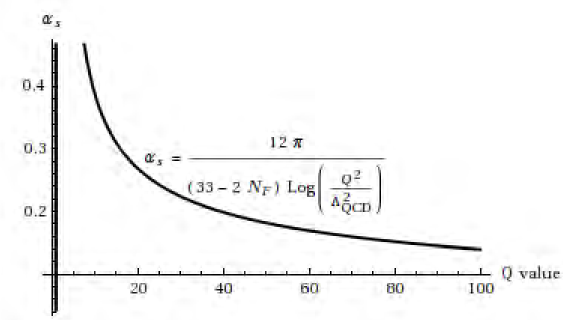

Figure 1.17: The plot of the variation of the running coupling constant of QCD as function of momentum.

these results one can conclude at high energy(closer to infinity) quarks are free. This is called asymptotic freedom and in low energy regime, quarks are not free. They are bound in the hadrons consisting of them. This is called confinement. Further more perturbation expansion is not applicable in low energy regime. Therefore, in low energy regime, we need nonperturbative treatment to consider hadronic processes. One of these nonperturbative methods is using Bethe-Salpeter equation. We derive Bethe Salpeter Equation(BSE) in the next chapter. The other nonperturbative approaches are: lattice gauge theories, potential models, chiral perturbation theory etc.

Chapter 2

Bethe Salpeter Equation

The Bethe-Salpeter equation describes the bound states of a two-body (particles) quantum mechanical system in a relativistically covariant formalism. Examples of two-particle systems described by the Bethe-Salpeter equation are positronium, bound state of an electron-positron pair. The Bethe-Salpeter formalism is generally accepted to represent the appropriate framework for the description of bound states within relativistic quantum field theory. Within this formalism, a bound state is described by its Bethe-Salpeter amplitude, which is defined as the time-ordered product of the field operators of the bound-state constituents between the vacuum and the bound state.

In principle, this bound-state amplitude should be found as a solution of the homogeneous Bethe-Salpeter equation. However, apart from a very few special cases such as the famous Wick-Cutkosky model which describes the interaction of two scalar particles by exchange of a massless scalar particle the Bethe-Salpeter equation turns out to be practically not tractable. One of the main reasons for this fact is the appearance of time-like variables in the equation of motion. Consequently people usually consider some three dimensional reduction of the Bethe-Salpeter equation. The most popular among these three-dimensional reductions is based on the assumption that the interaction between the bound-state constituents is instantaneous in the center-of momentum frame of the bound state. The result of this is called the "Salpeter equation" or "instantaneous Bethe- Salpeter equation". This equation may be formulated as eigenvalue problem for the mass M of the bound state. Its dynamical quantity is the "Salpeter amplitude," obtained from the Bethe-Salpeter amplitude by equating the time variables of the involved bound-state constituents. In this thesis we will employ a BSE formalism based on Covariant Instantaneous Ansatz(CIA) which is a Lorentz invariant generalization of Instantaneous Approximation(IA).

To derive the Bethe-Salpeter equation first it is necessary to start from the one particle Dirac propagator then generalizing to the two particle propagator.

2.1 Two Particle propagator

We know from propagator theory that one particle propagator in an external field can be expressed as an iteration series

$$K(x_1,x_2) = K_0(x_1,x_2) - e\int d^4x_3 K_0(x_1,x_3)\not{A}(x_3)(K_0(x_3,x_2)$$
$$+(-e)^2\int d^4x_3 d^4x_4 K_0(x_1,x_3)\not{A}(x_3)K_0(x_3,x_4)\not{A}(x_4)K(x_4,x_2) + ... \quad (2.1.1)$$

This is the propagator series equation for a one particle in an external field $A_\mu(x)$.

We now generalize the expression for the propagator obtained for one particle in an external field to two-particles in mutual interaction. The two particle propagator for simultaneous propagation of two non interacting particles, $K_{0ab}(x_1,x_2;x_3,x_4)$ can be written as the product of two single free propagators as,

$$K_{0ab}(x_1,x_2;x_3,x_4) = K_{0a}(x_1,x_3)K_{0b}(x_2,x_4). \quad (2.1.2)$$

To find the form of the propagator for these two-interacting particles, let us consider the simplest case(Moller interaction, $e^- + e^- \longrightarrow e^- + e^-$).

The two particles are governed by Coulomb interaction and the Coulomb potential is given by

$$V = \frac{e^2}{r_{ab}} \tag{2.1.3}$$

where $r_{ab} = r_a - r_b$ is the separation between them.

In Eq.(2.1.3) the Coulomb interaction potential is not in covariant form. To write it in a covariant form first $\frac{1}{r_{ab}}$ has to be transformed in to momentum space by Fourier transform. The Fourier transform of $\frac{1}{r}$ in momentum space is

$$\frac{1}{|r|} \longrightarrow \frac{1}{|p|^2}. \tag{2.1.4}$$

Therefore, the Fourier transform of $\frac{1}{r_{ab}}$ can be written as

$$\frac{1}{|r_{ab}|} \longrightarrow \frac{1}{(p_1 - p_1')^2}. \tag{2.1.5}$$

Still Eq.(2.1.5) is not in its covariant form. By introducing Dirac γ matrices, it is possible to write this potential covariantly as

$$\begin{aligned} V &= \frac{e^2\gamma_\mu^a\gamma_\mu^b}{(p_1 - p_1')^2}, \\ V &= -\gamma_\mu^a e^2(\frac{-1}{q^2})\gamma_\mu^b \end{aligned} \tag{2.1.6}$$

where q=$(p_1 - p_1')$. To generalize a single particle propagator for two particles propagator we replace

e$\gamma_\mu A_\mu \longrightarrow i\gamma_\mu^a e^2 D_F(x - x')\gamma_\mu^b$. For a single photon exchange between two interacting particles,

$$D_F(x - x') = \frac{-1}{(2\pi)^4}\int d^4q \frac{e^{iq.(x-x')}}{q^2}. \tag{2.1.7}$$

For a general case of one quantum exchange between two interacting particles in mutual interaction, D_F would be the corresponding gauge field propagator. That means D_F denotes the photon propagator in QED and the gluon propagator in QCD. The first order correction to two particles propagator for simultaneous propagation from space time point (x_3, x_4) to space time point (x_1, x_2) with the exchange of a single quantum will be

$$K_{1ab}(x_1, x_2; x_3, x_4) = \int d^4x_5 d^4x_6 K_{0ab}(x_1, x_2; x_5, x_6) I(x_5, x_6) K_{0ab}(x_5, x_6; x_3, x_4), \tag{2.1.8}$$

where $I(x_5, x_6) = ie_a e_b \gamma^a_\mu D_F(x_5, x_6)\gamma^b_\mu$. The letters a and b are indices for the two interacting particles. Here $I(x_5, x_6)$ plays the role of $\not{A}(x_3)$ in Eq.(2.1.1) for one particle propagator. The corresponding Feynman diagram to Eq.(2.1.8) is shown in Fig.(2.1).

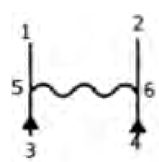

Figure 2.1: Feynman diagram to the first order correction for two interacting particles.

The second order correction to the two interacting particles propagator will be

$$\begin{aligned} K_{2ab}(x_1, x_2; x_3, x_4) &= \int d^4x_5 d^4x_6 d^4x_7 d^4x_8 K_{0ab}(x_1, x_2; x_5, x_6) I(x_5, x_6) \\ &\times K_{0ab}(x_5, x_6; x_7, x_8) I(x_7, x_8) K_{0ab}(x_7, x_8; x_3, x_4), \end{aligned} \tag{2.1.9}$$

and the corresponding Feynman diagram to Eq.(2.1.9) is shown in Fig.(2.2).

If we iterate only one quantum exchange as above, we arrive at an integral

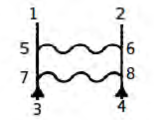

Figure 2.2: Feynman diagram to the second order correction for two interacting particles.

equation

$$
\begin{aligned}
&K_{ab}(x_1, x_2; x_3, x_4) = K_{0ab}(x_1, x_2; x_3, x_4) \\
&+ \int d^4x_5 d^4x_6 K_{0ab}(x_1, x_2; x_5, x_6) I(x_5, x_6) K_{0ab}(x_5, x_6; x_3, x_4) \\
&+ \int d^4x_5 d^4x_6 d^4x_7 d^4x_8 K_{0ab}(x_1, x_2; x_5, x_6) I(x_5, x_6) \\
&\times K_{0ab}(x_5, x_6; x_7, x_8) I(x_7, x_8) K_{0ab}(x_7, x_8; x_3, x_4) + ..., \qquad (2.1.10)
\end{aligned}
$$

which can be written as

$$K_{ab} = K_{0ab} + K_{1ab} + K_{2ab} + ... \qquad (2.1.11)$$

The corresponding Feynman diagram to Eq.(2.1.10) is shown in Fig.(2.3). Eq.(2.1.10)

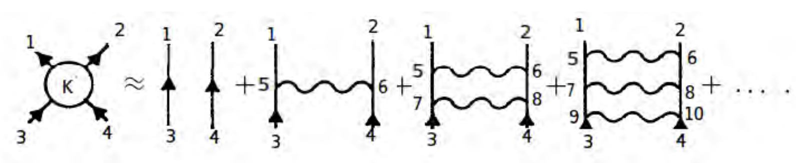

Figure 2.3: Ladder approximation diagram for two interacting particles.

can be written exactly as

$$
\begin{aligned}
&K_{ab}(x_1, x_2; x_3, x_4) = K_{0ab}(x_1, x_2; x_3, x_4) + \int d^4x_5 d^4x_6 K_{0ab}(x_1, x_2; x_5, x_6) I(x_5, x_6) \\
&\times K_{ab}(x_5, x_6; x_3, x_4). \qquad (2.1.12)
\end{aligned}
$$

2.2 Bethe-salpeter two-particle wave function

In non-relativistic quantum mechanics for a particle propagating from a space-time point $(\vec{r}', t')$ to a space-time $(\vec{r}, t)$, if the wave function at $(\vec{r}', t')$ is known, then the wave function at $(\vec{r}, t)$ is given by

$$\psi(\vec{r}, t) = \int d^3\vec{r}' K(\vec{r}, t; \vec{r}', t')\psi(\vec{r}', t'). \tag{2.2.13}$$

The above condition can be applied for a system of particles propagating simultaneously from space-time x_3, x_4 to space-time point x_1, x_2. That is if the wave function of the bound system at x_3, x_4 is known, then the wave function at x_1, x_2 can be given as

$$\psi(x_1, x_2) = \int d^3x_3 d^3x_4 K(x_1, x_2; x_3, x_4)\psi(x_3, x_4). \tag{2.2.14}$$

By substituting for $K(x_1, x_2; x_3, x_4)$ from Eq.(2.1.12) into Eq.(2.2.14) we obtain

$$\begin{aligned}\psi(x_1, x_2) = &\int d^3x_3 d^3x_4 [K_0(x_1, x_2; x_3, x_4) \\ &+ \int d^4x_5 d^4x_6 K_0(x_1, x_2; x_5, x_6) I(x_5, x_6) K(x_5, x_6; x_3, x_4)]\psi(x_3, x_4).\end{aligned} \tag{2.2.15}$$

Thus

$$\begin{aligned}\psi(x_1, x_2) = &\psi_0(x_1, x_2) + \int d^3x_3 d^3x_4 d^4x_5 d^4x_6 K_0(x_1, x_2; x_5, x_6) \\ &\times I(x_5, x_6) K(x_5, x_6; x_3, x_4)\psi(x_3, x_4).\end{aligned} \tag{2.2.16}$$

But

$$\int d^3x_3 d^3x_4 K(x_5, x_6; x_3, x_4)\psi(x_3, x_4) = \psi(x_5, x_6). \tag{2.2.17}$$

Substituting Eq.(2.2.17) into Eq.(2.2.16), one can obtain

$$\psi(x_1, x_2) = \psi_0(x_1, x_2) + \int d^4x_5 d^4x_6 K_0(x_1, x_2; x_5, x_6) I(x_5, x_6)\psi(x_5, x_6). \tag{2.2.18}$$

This is Bethe-Salpeter Equation. $\psi_0(x_1, x_2)$ is the free two particles wave function. BOUND STATE SYSTEMS:For bound states systems, $\psi_0(x_1, x_2)$ drops out of Eq.(2.2.18).

Thus for bound states, Eq.(2.2.18) will be reduced to

$$\psi(x_1, x_2) = \int d^4x_5 d^4x_6 K_0(x_1, x_2; x_5, x_6) I(x_5, x_6)\psi(x_5, x_6). \tag{2.2.19}$$

Eq.(2.2.19) can also be written in another form if one multiples with free Dirac operators $\gamma_\mu\partial_{1\mu}+m_1$ and $\gamma_\mu\partial_{2\mu}+m_2$. Multiplying Eq.(2.2.19) by $\gamma_\mu\partial_{1\mu}+m_1$ and $\gamma_\mu\partial_{2\mu}+m_2$ from the left, one can obtain

$$\begin{aligned}
&(\gamma_\mu\partial_{1\mu} + m_1)(\gamma_\mu\partial_{2\mu} + m_2)\psi(x_1, x_2) = \\
&(\gamma_\mu\partial_{1\mu} + m_1)(\gamma_\mu\partial_{2\mu} + m_2)\int d^4x_5 d^4x_6 K_0(x_1, x_2; x_5, x_6) \\
&I(x_5, x_6)\psi(x_5, x_6).
\end{aligned} \tag{2.2.20}$$

Since one particle propagators obey the relation

$$\begin{aligned}
(\gamma_\mu\partial_{1\mu} + m_1)K_0(x_1, x_5) &= -i\delta^{(4)}(x_1 - x_5), \\
(\gamma_\mu\partial_{2\mu} + m_2)K_0(x_2, x_6) &= -i\delta^{(4)}(x_2 - x_6)
\end{aligned} \tag{2.2.21}$$

it follows that

$$\begin{aligned}
&(\gamma_\mu\partial_{1\mu} + m_1)(\gamma_\mu\partial_{2\mu} + m_2)\psi(x_1, x_2) = \\
&\int d^4x_5 d^4x_6 (-i\delta^{(4)}(x_1 - x_5))(-i\delta^{(4)}(x_2 - x_6)) I(x_5, x_6)\psi(x_5, x_6).
\end{aligned} \tag{2.2.22}$$

Thus Eq.(2.2.19) becomes

$$(\gamma_\mu \partial_{1\mu} + m_1)(\gamma_\mu \partial_{2\mu} + m_2)\psi(x_1, x_2) = -I(x_1, x_2)\psi(x_1, x_2), \tag{2.2.23}$$

where $I(x_1, x_2) = ie^2 \gamma_\mu^a D(x_1, x_2)\gamma_\mu^b = iK(x_1, x_2)$. Now $K(x_1, x_2)$ is an interaction kernel and is given by $K(x_1, x_2) = e^2 \gamma_\mu^a D(x_1, x_2)\gamma_\mu^b$. Then the BSE can be written as

$$(\gamma_\mu \partial_{1\mu} + m_1)(\gamma_\mu \partial_{2\mu} + m_2)\psi(x_1, x_2) = -iK(x_1, x_2)\psi(x_1, x_2). \tag{2.2.24}$$

This is also another form of Bethe-Salpeter Equation(BSE) in coordinate representation. For practical purposes there is another useful form of this equation obtained by transforming it into momentum space. In the center-of-mass frame, the center of mass coordinate is given by

$$\bar{X} = \frac{m_1 x_1 + m_2 x_2}{m_1 + m_2}. \tag{2.2.25}$$

If we consider the condition $m_1 = m_2 = m$ then the center-of-mass coordinate becomes

$$\bar{X} = \frac{x_1 + x_2}{2} \tag{2.2.26}$$

and the relative separation between the two particles is also given by

$$x = x_1 - x_2. \tag{2.2.27}$$

From the above relation we can get

$$\begin{aligned} \partial_1 &= \frac{\partial}{\partial x_1} = \frac{\partial \bar{X}}{\partial x_1}\frac{\partial}{\partial \bar{X}} + \frac{\partial x}{\partial x_1}\frac{\partial}{\partial x} = \frac{1}{2}\partial_{\bar{X}} + \partial_x, \\ \partial_2 &= \frac{\partial}{\partial x_2} = \frac{\partial \bar{X}}{\partial x_2}\frac{\partial}{\partial \bar{X}} + \frac{\partial x}{\partial x_2}\frac{\partial}{\partial x} = \frac{1}{2}\partial_{\bar{X}} - \partial_x. \end{aligned} \tag{2.2.28}$$

Now by using $\bar{X}$ and x we can write $\psi(x_1, x_2)$ as follows. That is

$$\psi(x_1, x_2) = \psi(\bar{X})\psi(x), \tag{2.2.29}$$

where

$$\psi(\bar{X}) = \frac{1}{\sqrt{V}} e^{iP.\bar{X}}. \tag{2.2.30}$$

Substituting for $\psi(x_1, x_2)$ from equation (2.2.29) into equation (2.2.24), one can obtain

$$(\frac{1}{2}\not{\partial}_{\bar{X}\mu} + \not{\partial}_{x\mu} + m)(\frac{1}{2}\not{\partial}_{\bar{X}\mu} - \not{\partial}_{x\mu} + m)e^{iP.\bar{X}}\psi(x) = -iK(x)e^{iP.\bar{X}}\psi(x). \tag{2.2.31}$$

Differentiating with respect to $\partial_{\bar{X}}$, Eq.(2.2.31) will reduce to

$$(i\frac{1}{2}\not{P} + \not{\partial}_{x\mu} + m)(i\frac{1}{2}\not{P} - \not{\partial}_{x\mu} + m)\psi(x) = -iK(x)\psi(x). \tag{2.2.32}$$

where $\not{P}=\gamma_\mu P_\mu$ and P is the total momentum in the CM frame. Here in the above equation, $K(x)$ is taken as a function of x only. This is by assuming that the interaction between the particles depends on the relative separation between the two particles. Now by taking the inverse Fourier transform of $\psi(x)$ and $K(x)$ as

$$\begin{aligned}\psi(x) &= \frac{1}{(2\pi)^4}\int d^4q e^{iq.x}\psi(q),\\ K(x) &= \frac{1}{(2\pi)^4}\int d^4k e^{ik.x}K(k),\end{aligned} \tag{2.2.33}$$

where q is the relative momentum. Thus, Eq. (2.2.32)will be

$$\begin{aligned}&(\frac{1}{2}i\not{P} + \not{\partial}_{x\mu} + m)(\frac{1}{2}i\not{P} - \not{\partial}_{x\mu} + m)\frac{1}{(2\pi)^4}\int d^4q e^{iq.x}\psi(q)\\ &= \frac{-i}{(2\pi)^4}\int d^4q' e^{iq'.x}\psi(q')\frac{1}{(2\pi)^4}\int d^4k' e^{ik'.x}k(k').\\ &.\end{aligned} \tag{2.2.34}$$

Thus

$$(\frac{1}{2}i\not{P}+i\not{q}+m)(\frac{1}{2}i\not{P}-i\not{q}+m)\int d^4qe^{iq.x}\psi(q)$$
$$=\frac{-i}{(2\pi)^4}\int d^4q'd^4k'e^{i(q'+k').x}\psi(q')K(k'). \tag{2.2.35}$$

Let k'+q'=q for a given value of q'. Then $d^4k' = d^4q$. Therefore, the BSE in momentum space for bound state of two particles(with momenta p_1, p_2) and internal momentum q can be written as

$$(i\not{p}_1+m)(i\not{p}_2+m)\psi(q)=\frac{-i}{(2\pi)^4}\int d^4q'K(q-q')\psi(q'). \tag{2.2.36}$$

Eq.(2.2.36) is the Bethe-Salpeter Equation(BSE) in momentum representation(For some classic references on BSE see reference[13−16].

Bethe-Salpeter Equation(BSE) is notoriously difficult to solve. Finding the exact solution of the above equation is very difficult but one can approximate, say for example, using covariant Instantaneous Ansatz(CIA). We will deal this topic in the next section.

2.3 The Bethe-Salpeter Equation under CIA

We briefly outline the BSE framework under CIA. For simplicity, lets consider a $q\overline{q}$ system comprising of scalar quarks with an effective kernel K, 4D wave function $\Phi(P, q)$, the 4D BSE can be written as,

$$i(2\pi)^4\Delta_1\Delta_2\Phi(P,q)=\int d^4q'K(q,q')\Phi(P,q'), \tag{2.3.37}$$

where $\Delta_{1,2} = m_{1,2}^2 + p_{1,2}^2$ are the inverse propagators for the two quarks, and $m_{1,2}$ are (effective) constituent masses of quarks. The 4-momenta of the quark and anti-quark, $p_{1,2}$, are related to the internal 4-momentum q_μ and total momentum P_μ of hadron of mass M as $p_{1,2\mu} = \widehat{m}_{1,2}P_\mu \pm q_\mu$, where $\widehat{m}_{1,2} = [1 \pm (m_1^2 - m_2^2)/M^2]/2$ are the Wightman-Garding (WG) definitions of masses of individual quarks. Now it is convenient to express the internal momentum of the hadron q as the sum of two parts, the transverse component, $\hat{q}_\mu = q_\mu - \frac{q.P}{P^2}P_\mu$ which is orthogonal to total hadron momentum P (ie. $\widehat{q}.P = 0$ regardless of whether the individual quarks are on-shell or off-shell), and the longitudinal component, $\sigma P_\mu = (q \cdot P/P^2)P_\mu$, which is parallel to P. To obtain Hadron-quark vertex, use an Ansatz on the BS kernel K in Eq. (2.3.38) which is assumed to depend on the 3D variables $\hat{q}_\mu$, $\hat{q}'_\mu$ [17−21] i.e.

$$K(q, q') = K(\hat{q}, \hat{q}'), \tag{2.3.38}$$

(A similar form of the BS kernel was also earlier suggested in ref. [22]. Hence, the longitudinal component, σP_μ of q_μ , does not appear in the form $K(\hat{q}, \hat{q}')$ of the kernel. For reducing Eq.(2.3.37) to the 3D form of BSE, we define a 3D wave function $\phi(\hat{q})$ as,

$$\phi(\hat{q}) = \int_{-\infty}^{+\infty} M d\sigma \Phi(P, q). \tag{2.3.39}$$

Substituting Eq.(2.3.39) in Eq.(2.3.37), with the definition of the kernel in Eq.(2.3.38), we get a covariant version of the Salpeter equation which is in fact a 3D BSE:

$$(2\pi)^3 D(\hat{q})\phi(\hat{q}) = \int d^3\hat{q}' K(\hat{q}, \hat{q}')\phi(\hat{q}'). \tag{2.3.40}$$

Here $D(\hat{q})$ is the 3D denominator function defined below whose value is obtained by evaluating contour integration over inverse quark propagators in the complex σ-plane by noting their corresponding pole positions [18–20] as,

$$\frac{1}{D(\hat{q})} = \frac{1}{2\pi i}\int_{-\infty}^{+\infty}\frac{Md\sigma}{\Delta_1\Delta_2} = \frac{\frac{1}{2\omega_1}+\frac{1}{2\omega_2}}{(\omega_1+\omega_2)^2-M^2}, \omega_{1,2}^2 = m_{1,2}^2+\hat{q}^2. \tag{2.3.41}$$

Since the (Left hand side) LHS of Eq.(2.3.37) is independent of q' and $d^4q' = d^3\widehat{q'}M'd\sigma'$, we can perform the pole integration over $M'd\sigma'$ in the right hand side (RHS) of Eq.(2.3.37) which is equal to the RHS of Eq.(2.3.40). Thus, the LHS of Eq.(2.3.37) is exactly identical to the LHS of Eq.(2.3.40) by virtue of Eq.(2.3.38) and Eq.(2.3.39). We thus have an exact interconnection between 3D BSE and the 4D BSE, and hence between the 3D wave function $\phi(\hat{q})$ and the 4D wave function $\Phi(P,q)$[17–20]:

$$\Delta_1\Delta_2\Phi(P,q) = \frac{D(\hat{q})\phi(\hat{q})}{2\pi i} \equiv \Gamma(\hat{q}), \tag{2.3.42}$$

where $\Gamma(\hat{q})$ is the Bethe-Salpeter Hadron-quark vertex function for a meson comprising of scalar quarks.

The 4D BS wave function $\Phi(P,q)$ can be reconstructed from the 3D BS wave function $\phi(\hat{q})$ as:

$$\Phi(P,q) = \frac{1}{\Delta_1}\Gamma(\hat{q})\frac{1}{\Delta_2}, \tag{2.3.43}$$

where $\Delta_i = (m_i^2+p_i^2)$,(i=1,2) are the inverse propagators for scalar quarks which flank the hadron-quark vertex Γ. This 4D hadron-quark vertex $\Gamma(\hat{q})$ satisfies a 4D BSE with a natural off-shell extension over the entire 4D space (due to the positive definiteness of the quantity $\hat{q}^2 = q^2-(q\cdot P)^2/P^2$ throughout the entire 4D space) and thus provides a fully Lorentz-invariant basis for evaluation of various transition amplitudes through various quark loop diagrams. Due to these properties, this framework of BSE under CIA can be profitably employed not only for low energy studies but also for evaluation of various transition amplitudes at quark level all the way from low energies to high energies. However this 4D hadron-quark vertex Γ is still unnormalized and can be normalized as will be shown in the realistic case of fermionic quarks next.

For fermionic quarks the BSE under CIA can be written as:

$$i(2\pi)^4\Psi(P,q) = S_{F1}(p_1)S_{F2}(-p_2)\int d^4q' K(\widehat{q},\widehat{q'})\Psi(P,q'), \tag{2.3.44}$$

where the scalar propagators Δ_i^{-1} in the above equations are replaced by fermionic propagators S_F. Further the $Hq\bar{q}$ vertex would be a 4×4 matrix in the spinor space for which we should incorporate the relevant Dirac structures. For incorporation of the relevant Dirac structures in $\Gamma(\hat{q})$, they are incorporated order-by-order in powers of inverse of meson mass M, in accordance with the power counting rule developed in reference [(19)]. The aim of developing the power counting rule was to find a "criterion" so as to systematically choose among various Dirac covariant from their complete set to write wave functions for different meson (vector meson, pseudoscalar meson etc.)[(19,20)]. In another recent work, leptonic decay constants of unequal mass pseudoscalar meson like π, K, D, D_s and B and radiative decays of equal mass pseudoscalar meson like π^0, η_c were studied by taking into account both the leading order (LO) and Next-to-Leading Order (NLO) Dirac covariant and relevance of various Dirac covariants in decay calculation was studied. It was found that the contribution of leading order (LO) covariant to decay constants was maximum (about 90-95 percent) for heavier meson composed of c and b quarks like D, D_s, B and η_c(for details see reference [(21)]), while there was little contribution from NLO covariants. Among the LO covariant, it was also noticed that for pseudoscalar meson, the contribution from covariant, γ_5 was maximum and similarly for vector meson, the contribution of

LO covariant $i\gamma.\varepsilon$ was maximum. This was our motivation to use these most leading covariants in our calculations such as $(i)e^+ + e^- \rightarrow J/\psi, (ii)h \rightarrow h' + \gamma$ and $(iii)h \rightarrow h' + h$" in this thesis. The full fledged normalized 4D BS wave functions for a $q\bar{q}$ meson with quarks total momentum P and relative momentum q and with individual quarks with momenta p_1 and p_2 can be written as:

$$\Psi(P, q) = S_F(p_1)\Gamma(\hat{q})S_F(-p_2) \tag{2.3.45}$$

where the 4D BS hadron-quark vertex function which absorbs the 4D BS normalizer N is,

$$\Gamma(\hat{q}) = N\Gamma_i D(\hat{q})\phi(\hat{q})/2\pi i \tag{2.3.46}$$

where $\Gamma_i = \gamma_5, i\gamma.\varepsilon, ...$ are the relevant Dirac structures for pseudoscalar mesons, vector mesons etc. The 4D BS normalizer N which is determined from standard current conserving conditions and is worked out in the framework of Covariant Instantaneous Ansatz (CIA) to give explicit covariance to the full fledged 4D BS wave function, $\Psi(P, q)$ and hence to the Hadron-quark vertex function, $\Gamma(\hat{q})$ employed for calculation of transition amplitudes at high energies.

Thus the 4D hadron-quark vertex function for Pseudoscalar meson is,

$$\Gamma^P(\widehat{q}) = \gamma_5 N_P D(\widehat{q})\phi(\widehat{q})/2\pi i, \tag{2.3.47}$$

while the 4D hadron-quark vertex function for vector meson is,

$$\Gamma^V(\widehat{q}) = i\gamma.\varepsilon N_V D(\widehat{q})\phi(\widehat{q})/2\pi i. \tag{2.3.48}$$

Here $D(\widehat{q})$ is the denominator function, and $\phi(\widehat{q})$ is the 3D BS wave functions for the meson, while ε is the polarization vector for the vector meson, N_P and N_V are the 4D

BS normalizers for Pseudoscalar and vector meson respectively which are determined through the current conservation condition which is given by[17−21]

$$2iP_\mu = (2\pi)^4 \int d^4q Tr[\overline{\Psi}(P,q)\frac{\partial}{\partial P_\mu}S_F^{-1}(p_1)\Psi(P,q)S_F^{-1}(-p_2)] + (1 \leftrightarrows 2). \qquad (2.3.49)$$

As far as the input kernel $K(q,q')$[17−21], in BSE is concerned, it is taken as one-gluon-exchange like as regards color $[(\lambda^{(1)}/2)\cdot(\lambda^{(2)}/2)]$ and spin $(\gamma_\mu^{(1)}\gamma_\mu^{(2)})$ dependence. The scalar function $V(q-q')$ is a sum of one-gluon exchange V_{OGE} and a confining term V_{conf}. Thus we can write the interaction kernel as [17−21]:

$$K(q,q') = \left(\frac{1}{2}\lambda^{(1)}\right)\cdot\left(\frac{1}{2}\lambda^{(2)}\right) V_\mu^{(1)}V_\mu^{(2)}V(q-q'),$$

$$V_\mu^{(1,2)} = \pm 2m_{1,2}\gamma_\mu^{(1,2)},$$

$$\begin{aligned} V(\hat{q}-\hat{q}') &= \frac{4\pi\alpha_S(Q^2)}{(\hat{q}-\hat{q}')^2} + \frac{3}{4}\omega_{q\bar{q}}^2\int d^3r\left[r^2(1+4a_0\hat{m}_1\hat{m}_2M^2r^2)^{-1/2} - \frac{C_0}{\omega_0^2}\right]e^{i(\hat{q}-\hat{q}')\cdot r}, \\ \alpha_S(Q^2) &= \frac{12\pi}{33-2f}\left(\ln\frac{Q^2}{\Lambda^2}\right)^{-1}. \end{aligned} \qquad (2.3.50)$$

The Ansatz employed for the spring constant $\omega_{q\bar{q}}^2$ in Eq. (2.3.50) is [17−21],

$$\omega_{q\bar{q}}^2 = 4\widehat{m}_1\widehat{m}_2M_>\omega_0^2\alpha_S(M_>^2), \quad M_> = Max(M, m_1+m_2). \qquad (2.3.51)$$

Here $\widehat{m}_1$, $\widehat{m}_2$ are the Wightman-Garding definitions of masses of constituent quarks defined earlier. Here the proportionality of $\omega_{q\bar{q}}^2$ on $\alpha_S(Q^2)$ is needed to provide a more direct QCD motivation to confinement. This assumption further facilitates a flavor variation in $\omega_{q\bar{q}}^2$. And ω_0^2 in Eq. (2.3.50) and Eq. (2.3.51) is postulated as a universal spring constant which is common to all flavors. Here in the expression for $V(\hat{q}-\hat{q}')$, as far as the integrand of the confining term V_{conf} is concerned, the constant term C_0/ω_0^2 is designed to take account of the correct zero point energies, while a_0 term ($a_0 \ll 1$) simulates an effect of an almost linear confinement for heavy quark sectors (large m_1, m_2), while retaining the harmonic form for light quark sectors (small m_1, m_2) [17−21] as is believed to be true for QCD. Hence the term $r^2(1+4a_0\widehat{m}_1\widehat{m}_2M_>^2r^2)^{-1/2}$ in the above expression is responsible for effecting a smooth transition from harmonic ($q\overline{q}$) to linear ($Q\overline{Q}$) confinement . The values of basic constants are: $C_0 = .29$, $\omega_0 = 0.158$ GeV, $m_{u,d} = 0.265$ GeV, $m_s = 0.415$ GeV, $m_c = 1.530$ GeV and $m_b = 4.900$ GeV which have been earlier fit to the mass spectrum of $q\overline{q}$ meson[17] obtained by solving the 3D BSE under Null-Plane Ansatz (NPA). However due to the fact that the 3D BSE under CIA has a structure which is formally equivalent to the 3D BSE under NPA, near the surface $P.q = 0$, the $q\overline{q}$ mass spectral results in CIA formalism are exactly the same as the corresponding results under NPA formalism[17,18,23]. The details of BS model under CIA in respect of spectroscopy are thus directly taken over from NPA formalism (For details see reference [17,23]). As far as the 3D wave function $\phi(\hat{q})$ is concerned, it satisfies the 3D BSE on the surface P.q=0, which is appropriate for making contact with the mass spectra [17]). Its fuller structure is reducible to that of a 3D harmonic oscillator. The ground state wave function deducible from this equation has a gaussian structure and is expressible as $\phi(\hat{q}) \approx e^{-\hat{q}^2/2\beta^2}$, where β is the inverse range parameter which incorporates the content of BS dynamics and is dependent on the input kernel and is given as [17,19,20]:

$$\beta^2 = (2\widehat{m}_1\widehat{m}_2M\omega_{q\bar{q}}^2/\gamma^2)^{1/2}, \gamma^2 = 1 - \frac{2\omega_{q\bar{q}}^2C_0}{M_>\omega_0^2}. \tag{2.3.52}$$

2.4 BS normalizer N_P and N_V

The BS normalizer N_P for pseudoscalar mesons and N_V for vector mesons are determined from the current conservation condition which is given by

$$\frac{2iP_\mu}{(2\pi)^4} = \int d^4qTr[\overline{\Psi}(P,q)\frac{\partial}{\partial P_\mu}S_F^{-1}(p_1)\Psi(P,q)S_F^{-1}(-p_2)] + (1 \Longleftrightarrow 2.) \tag{2.4.53}$$

We consider first the pseudoscalar case and followed by vector case.

2.4.1 Pseudoscalar meson normalizer N_P

Substituting Eq.(2.3.45) and Eq.(2.3.47) in Eq.(2.4.53), one can obtain

$$\frac{2iP_\mu}{(2\pi)^4} = \frac{N_P^2}{(2\pi i)^2}\int d^4qD^2(\widehat{q})\phi^2(\widehat{q})Tr[S_F(-p_2)\gamma_5S_F(p_1)\frac{\partial}{\partial P_\mu}S_F^{-1}(p_1)S_F(p_1)\gamma_5S_F(-p_2)$$
$$S_F^{-1}(-p_2)] + (1 \Longleftrightarrow 2.) \tag{2.4.54}$$

To simplify the above equation, note that

$$\frac{\partial}{\partial P_\mu}S_F^{-1}(\pm p_{1,2}) = \pm i\gamma_\mu\widehat{m}_{1,2} + i\gamma_\mu\sigma, S_F(-p_2)S_F^{-1}(-p_2) = -i \tag{2.4.55}$$

and

$\mathrm{S}_F(\pm p_i) = -i\frac{\mp i\gamma.p_i+m_i}{\Delta_i}$,

where $\Delta_i = p_i^2 + m_i^2$ and i stands for the quark number in the mesons. Substituting the above expressions in Eq.(2.4.54), one can obtain

$$\frac{2iP_\mu}{(2\pi)^4} = i\frac{N_P^2}{(2\pi i)^2}\int d^4q\frac{D^2(\widehat{q})\phi^2(\widehat{q})}{\Delta_1^2\Delta_2}(\widehat{m}_1+\sigma)Tr[TR] + (1 \Longleftrightarrow 2,) \tag{2.4.56}$$

where [TR] is the trace over the product of the gamma matrices coming from the hadron- quark vertex functions for the meson and the internal quark propagators, and can be expressible as

$$\begin{aligned}Tr[TR] &= Tr[(i\gamma.p_2+m_2)\gamma_5(-i\gamma.p_1+m_1)\gamma_\mu(-i\gamma.p_1+m_1)\gamma_5]\\ &= 4i[2(p_1.p_2-m_1m_2)p_{1\mu}-\Delta_1 p_{2\mu}].\end{aligned} \quad (2.4.57)$$

Since $p_1+p_2=P$, where P is the total momentum, one can obtain $2p_1.p_2 = P^2-p_1^2-p_2^2 = P^2-\Delta_1-\Delta_2+m_1^2+m_2^2$ and then

$$Tr[(i\gamma.p_2+m_2)\gamma_5(-i\gamma.p_1+m_1)\gamma_\mu(-i\gamma.p_1+m_1)\gamma_5] = 4i[(P^2-\Delta_2+\delta m^2)p_{1\mu}-\Delta_1 P_\mu], \quad (2.4.58)$$

where $\delta m = m_1-m_2$. When 1 replaced by 2, $p_{1\mu}\to p_{2\mu}, \Delta_1\to\Delta_2$, and $\widehat{m}_1+\sigma\to\widehat{m}_2-\sigma$ and thus $Tr[...]_{1\to 2} = 4i[2(p_1.p_2-m_1m_2)p_{2\mu}-\Delta_2 p_{1\mu}]$, or $Tr[...]_{1\to 2} = 4i[(P^2-\Delta_1+\delta m^2)p_{2\mu}-\Delta_2 P_\mu]$. Therefore, Eq.(2.4.56) becomes

$$\begin{aligned}2iP_\mu = \quad & 16\pi^2 N_P^2\int d^4q D^2(\widehat{q})\phi^2(\widehat{q})[\frac{(\widehat{m}_1+\sigma)((P^2-\Delta_2+\delta m^2)p_{1\mu}-\Delta_1 P_\mu)}{\Delta_1^2\Delta_2}\\ &+\frac{(\widehat{m}_2-\sigma)((P^2-\Delta_1+\delta m^2)p_{2\mu}-\Delta_2 P_\mu)}{\Delta_1\Delta_2^2}].\end{aligned} \quad (2.4.59)$$

Multiply both sides of the preceding equation by P_μ and divide both sides by M^2, one can obtain

$$\begin{aligned}N_P^{-2} = \quad & \frac{8i\pi^2}{M^2}\int d^4q D^2(\widehat{q})\phi^2(\widehat{q})[\frac{(\widehat{m}_1+\sigma)((P^2-\Delta_2+\delta m^2)P.p_1-\Delta_1 P^2)}{\Delta_1^2\Delta_2}\\ &+\frac{(\widehat{m}_2-\sigma)((P^2-\Delta_1+\delta m^2)P.p_2-\Delta_2 P^2)}{\Delta_1\Delta_2^2}].\end{aligned} \quad (2.4.60)$$

To simplify let us consider equal mass case, i.e., $m_1=m_2=m, \widehat{m}_1=\widehat{m}_2=\frac{1}{2}$. In terms of the total momentum, P and relative momentum, q, $p_1=\frac{P}{2}+q$, $p_2=\frac{P}{2}-q$ and hence

$$P.p_1 = -M^2(\frac{1}{2}+\sigma), P.p_2 = -M^2(\frac{1}{2}-\sigma). \quad (2.4.61)$$

Substituting Eq.(2.4.61) into Eq.(2.4.60) and since $d^4q = 4\pi\widehat{q}^2 d\widehat{q} M d\sigma$, one can obtain

$$N_P^{-2} = \frac{32i\pi^3}{M^2}\int M d\sigma d^3\widehat{q} D^2(\widehat{q})\phi^2(\widehat{q})\left[\frac{(\frac{1}{2}+\sigma)(M^2(M^2+\Delta_2)(\frac{1}{2}+\sigma)+\Delta_1 M^2)}{\Delta_1^2\Delta_2}\right.$$
$$\left.+\frac{(\frac{1}{2}-\sigma)(M^2(M^2+\Delta_1)(\frac{1}{2}-\sigma)+\Delta_2 M^2)}{\Delta_1\Delta_2^2}\right]. \tag{2.4.62}$$

Unfortunately the $(\frac{1}{2}+\sigma)^2$ and $(\frac{1}{2}-\sigma)^2$ in the numerator cause a negative contribution to the $\sigma-$ integration. To overcome this problem, one may consider, following reference [17], that the 'charge' is concentrated on one of the quark lines, say p_1, which amounts to taking the derivative w.r.t. p_1 instead of w.r.t. P as above. A more symmetrical possibility consists in interchanging p_1 with p_2, and weighing these two contributions with the momentum fractions $\widehat{m}_{1,2}$, respectively . The result for the pseudoscalar case, after simplification

$$N_P^{-2} = \frac{32i\pi^3}{M^2}\int M d\sigma d^3\widehat{q} D^2(\widehat{q})\phi^2(\widehat{q})\left[\frac{M^2(M^2+\Delta_2)(\frac{1}{2}+\sigma)+\Delta_1 M^2}{\Delta_1^2\Delta_2}\right.$$
$$\left.+\frac{M^2(M^2+\Delta_1)(\frac{1}{2}-\sigma)+\Delta_2 M^2}{\Delta_1\Delta_2^2}\right]. \tag{2.4.63}$$

Since $\Delta_1 = -M^2(\sigma+\frac{1}{2})^2+\omega^2, \Delta_2 = -M^2(\sigma-\frac{1}{2})^2+\omega^2$, where $\omega^2 = \widehat{q}^2+m^2$ we can perform the pole integration over σ and thus the integrand will be a function of $\widehat{q}$. Hence, the numerical value of the BS normalizer is, therefore, obtained from the above equation by performing numerical integration over $\widehat{q}$.

2.4.2 Vector meson normalizer N_V

The vector meson normalizer N_V is obtained from Eq.(2.4.56) by replacing γ_5 by $i\gamma.\epsilon$ before evaluating the trace. ϵ is the spin polarization vector of the vector meson. Thus,

$$\frac{2iP_\mu}{(2\pi)^4} = i\frac{N_V^2}{(2\pi i)^2}\int d^4q\frac{D^2(\widehat{q})\phi^2(\widehat{q})}{\Delta_1^2\Delta_2}2\widehat{m}_1 Tr[TR] + (1 \Longleftrightarrow 2,) \tag{2.4.64}$$

where [TR] is the trace over the product of the gamma matrices coming from the hadron- quark vertex functions for the meson and the internal quark propagators, and can be expressible as

$$Tr[TR] = Tr[(i\gamma.p_2 + m_2)i\gamma.\epsilon(-i\gamma.p_1 + m_1)\gamma_\mu(-i\gamma.p_1 + m_1)i\gamma.\epsilon]$$
$$= 8i(-2p_2.\epsilon p_1.\epsilon p_{1\mu} + \Delta_1 p_2.\epsilon\epsilon_\mu) - 8im_1m_2p_{1\mu} - 4(-p_1.p_2p_{1\mu} + \Delta_1 p_{2\mu}) \tag{2.4.65}$$

The second term corresponding to ($1 \Longleftrightarrow 2$) leads to,

$$Tr[(i\gamma.p_2 + m_2)i\gamma.\epsilon(-i\gamma.p_1 + m_1)\gamma_\mu(-i\gamma.p_1 + m_1)i\gamma.\epsilon]_{1\to 2}$$
$$= 8i(-2p_2.\epsilon p_1.\epsilon p_{2\mu} + \Delta_2 p_1.\epsilon\epsilon_\mu) - 8im_1m_2p_{2\mu} - 4(-p_1.p_2p_{2\mu} + \Delta_2 p_{1\mu}) \tag{2.4.66}$$

Following a logical sequence of steps we can express the v meson result analogous to Eq.(2.4.63) as

$$\begin{aligned} N_V^{-2} = \quad & \frac{32i\pi^3}{M^2}\int Md\sigma d^3\widehat{q}D^2(\widehat{q})\phi^2(\widehat{q})[\frac{M^2(M^2 - \frac{2}{3}\widehat{q}^2 + \Delta_2)(\frac{1}{2}+\sigma) + \Delta_1 M^2}{\Delta_1^2\Delta_2} \\ & + \frac{M^2(M^2 - \frac{2}{3}\widehat{q}^2 + \Delta_1)(\frac{1}{2}-\sigma) + \Delta_2 M^2}{\Delta_1\Delta_2^2}]. \end{aligned} \tag{2.4.67}$$

In the trace calculation we have also average over the vector meson polarization according to

$$< \epsilon_\mu\epsilon_\nu >= \frac{1}{3}\Theta_{\mu\nu}, \Theta_{\mu\nu} = \delta_{\mu\nu} + \frac{P_\mu P_\nu}{M^2}. \tag{2.4.68}$$

Analytic integrations over $d\sigma$ are first performed in the complex σ-plane by noting the corresponding pole positions of Δs. Then numerical integration over $d^3\widehat{q}$ is performed giving numerical results for N_P and N_V.

Chapter 3

Application of BSE under CIA to calculate the cross section for double charmonium production in electron-positron annihilation at energy $\sqrt{s}$= 10.6 GeV

The exclusive production of a pair of doubly heavy mesons with c-quarks in e^+e^- annihilation at B-factories has attracted considerable attention in the last years. This is due to the fact that the cross section of the process $e^+ + e^- \to J/\psi + \eta_c$ at center of mass energy 10.6GeV which was measured in the experiments on Babar[(24)] and Belle detectors[(25,26)] at the energy $\sqrt{s}$ = 10.6 GeV has great discrepancy with the theoretical predictions.

To reduce the discrepancy many efforts have been made. For example, as discussed in[(27)], corrections from pure electromagnetic interactions are introduced into the non-relativistic QCD (NRQCD) factorization formalism. The next-to-leading order contributions of strong interaction are taken into account in[(28,29)]. In[(30)],the authors take into account corrections to the J/ψ leptonic decay width and the scale dependence of the leading-order prediction; etc.

Discussions given in reference [28,29] suggest that to reduce the large discrepancy between the experimental results and the theoretical predictions based on NRQCD for the process $e^-e^+ \to J/\psi + \eta_c$ with the final state which is composed of two charmonia, large next-to-leading-order (NLO) corrections may appear (the 'NLO' contribution is about 1.8 to 2.1 times of the leading-order one). Including this large NLO contributions, their results are close to the lower bound set by the Babar and Belle collaborations for the double-charmonia production. The authors also indicate that including the relativistic corrections can further enhance the estimated value.

In the present work done in this thesis, by properly including relativistic effects, we try to calculate the cross section for the process of double heavy quarkonium production $e^-e^+ \to J/\psi + \eta_c$ by applying the two-particle Bethe-Salpeter (BS) wave equation. The BS equation is in principle established in the frame work of relativistic quantum field theory. Therefore, it is supposed to include all relativistic effects. We make use of BSE under CIA to solve this problem. In order to simplify the calculation we will use the heavy quark approximation($q \ll M$) which is only intended to simplify the loop integrals. However, we do not employ the non covariant heavy quark limit.

3.1 Calculation of amplitude and cross section for the process $e^+ + e^- \longrightarrow J/\Psi + \eta_c$

There are four Feynman diagrams in the leading order (LO) of QCD for the process $e^+ + e^- \longrightarrow J/\Psi + \eta_c$. Two of these are depicted in Fig.3.1. The other two diagrams can be obtained by permutations. The details of momentum labeling of Fig.3.1a is shown in Fig.3.2 below. With reference to the momentum labeling in Fig.3.2, the adjoint BS wave function for η_c meson can be written down as:

$$\overline{\Psi}(P_b, q_b) = S_F(-q_2)\Gamma^P(\widehat{q}_b)S_F(q_4), \tag{3.1.1}$$

while for J/ψ meson, the adjoint BS wave function can be written as:

$$\overline{\Psi}(P_a, q_a) = S_F(-q_3)\Gamma^V(\widehat{q}_a)S_F(q_1'), \tag{3.1.2}$$

where q_a, q_b are the internal momenta of the hadrons J/Ψ and η_c respectively with the corresponding hadron-quark vertex functions Γ^V and Γ^P given in Eq.(2.3.47) and Eq.(2.3.48).

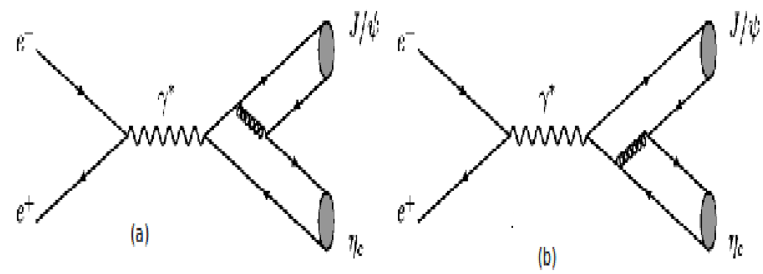

Figure 3.1: Two of the lowest order Feynman diagrams for the production of a pair of doubly heavy $c\bar{c}$ mesons in e^+e^- annihilation. Other two diagrams can be obtained by permutations.

Using Feynman rules, one can obtain the amplitude for each of the diagrams in Fig.3.1. The scattering amplitude corresponding to process in Fig.3.1a (described in detail in Fig.3.2) is given by

$$\begin{aligned}
S_{fi} &= \frac{m_e}{E_e V}\frac{1}{(2\pi)^{12}}\int d^4q d^4q_1 d^4k d^4q_1' d^4q_2 d^4q_3 d^4q_4 \overline{v}^{(s_2)}(\overrightarrow{p}_2)(ie\gamma_\mu)u^{(s_1)}(\overrightarrow{p}_1)(\frac{-i\delta_{\mu\nu}}{q^2})) \\
&\times Tr[TR]\frac{\lambda_a\lambda_a}{4}(\frac{-i\delta_{\alpha\beta}}{k^2})(2\pi)^{16}\delta^4(p_1+p_2-q)\delta^4(q-q_1-q_2)\delta^4(q_1-k-q_1') \\
&\times \delta^4(k-q_3-q_4)\delta^4(P_a-q_1'-q_3)\delta^4(P_b-q_2-q_4),
\end{aligned} \tag{3.1.3}$$

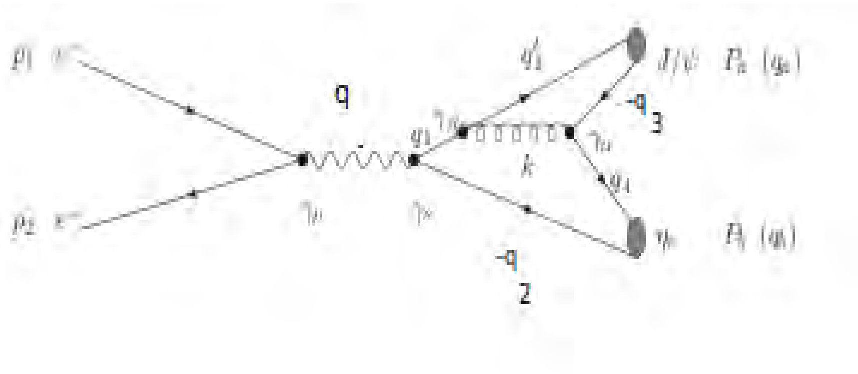

Figure 3.2: Momentum labeling of the first of the two Feynman diagrams shown in Fig.3.1

where

$$Tr[TR] = Tr[\overline{\Psi}(P_a, q_a)\gamma_\beta S_F(q_1)\gamma_\nu \overline{\Psi}(P_b, q_b)\gamma_\alpha]. \quad (3.1.4)$$

After integrating the above equation over q, q_1, and k, one can obtain

$$S_{fi} = \frac{m_e}{E_e V}\frac{1}{(2\pi)^{12}}\int d^4q_1' d^4q_2 d^4q_3 d^4q_4 \overline{v}^{(s_2)}(\overrightarrow{p}_2)(ie\gamma_\mu)u^{(s_1)}(\overrightarrow{p}_1)(\frac{-i\delta_{\mu\nu}}{q^2}))$$
$$\times Tr[TR]\frac{\lambda_a\lambda_a}{4}(\frac{-i\delta_{\alpha\beta}}{k^2})(2\pi)^{16}\delta^4(P_a - q_1' - q_3)\delta^4(P_b - q_2 - q_4)$$
$$\delta^4(p_1 + p_2 - q_1' - q_3 - q_2 - q_4). \quad (3.1.5)$$

To integrate the above equation over momenta q_1', q_2, q_3, and q_4, it is useful expressing these momenta in terms of the total momenta $P_{a(b)}$ and relative momenta $q_{a(b)}$. Thus, in terms $P_{a(b)}$ and $q_{a(b)}$, $d^4q_1' d^4q_3 = d^4P_a d^4q_a$, and $d^4q_2 d^4q_4 = d^4P_b d^4q_b$. Using these relations in the above equation and integrating over d^4P_a, and d^4P_b, one can obtain

$$S_{fi} = (2\pi)^4\delta^4(p_1 + p_2 - P_a - P_b)M_{fi}, \tag{3.1.6}$$

where M_{fi} is the scattering matrix element and is given by

$$M_{fi} = \frac{m_e}{E_e V} c\delta_{\mu\nu} e e_Q g_s^2 \frac{1}{s}\overline{v}(p_2)\gamma_\mu u(p_1)\int d^4q_a d^4q_b Tr[\overline{\Psi}(P_a, q_a)\gamma_\beta S_F(q_1)\gamma_\nu \overline{\Psi}(P_b, q_b)\gamma_\alpha]\frac{\delta_{\alpha\beta}}{k^2} \tag{3.1.7}$$

which can in turn be expressed as,

$$\begin{aligned} M_{fi} = \quad & \frac{m_e}{E_e V}\frac{c\delta_{\mu\nu} e e_Q g_s^2}{s}\overline{v}(p_2)\gamma_\mu u(p_1)\int d^4q_a d^4q_b \\ & \times Tr[S_F(-q_3)\Gamma_v(\hat{q}_a)S_F(q_1')\gamma_\beta S_F(q_1)\gamma_\nu S_F(-q_2)\Gamma_p(\hat{q}_b)S_F(q_4)\gamma_\alpha]\frac{\delta_{\alpha\beta}}{k^2} \end{aligned} \tag{3.1.8}$$

where c $=\frac{4}{3}$ is the color factor, the Mendelstam variable s is defined as, $s = -(p_1+p_2)^2$ and $e_Q = 2e/3$ is the electric charge of the charmed quark. The momentum relations of the quark and anti-quark in the final state are:

$$q_1' = \frac{1}{2}P_a + q_a, q_3 = \frac{1}{2}P_a - q_a, q_4 = \frac{1}{2}P_b + q_b, q_2 = \frac{1}{2}P_b - q_b, \tag{3.1.9}$$

and the momenta in the gluon and the quark propagators are given by

$$k = q_3 + q_4 = \frac{1}{2}(P_a + P_b) - q_a + q_b, \tag{3.1.10}$$

$$q_1 = q_1' + k = P_a + \frac{1}{2}P_b + q_b, \tag{3.1.11}$$

respectively. As each of quark momenta in the quark propagators as well as the gluon propagator is going to depend upon the internal hadron momenta q_a and q_b, the calculation of amplitude is going to involve integrations over these internal momenta and will be quite complex. Hence, we simplify the calculation, by employing the heavy quark approximation on the quark propagators, where we take the quark masses to be much larger than the internal momenta q_a and q_b of the hadrons. In this heavy quark approximation,we can use the approximation, $q_a << M_a, q_b << M_b$. Thus we can write,

$$q_{a(b)} \ll P_{a(b)} \sim M_{a(b)}, k = \frac{1}{2}(P_a + P_b) - q_a + q_b \approx \frac{1}{2}(P_a + P_b),$$
$$q_1 = P_a + \frac{1}{2}P_b + q_b \approx P_a + \frac{1}{2}P_b. \tag{3.1.12}$$

With the above approximation, k^2 and q_1^2 are given by $k^2 \approx -\frac{s}{4}$ and $q_1^2 \approx -\frac{s}{2} - m_c^2$. The propagators for the quarks and anti-quarks in momentum space are given by $S_F(q_i) = \frac{-i}{i\gamma.q_i+m_c} = \frac{-i(-i\gamma.q_i+m_c)}{\Delta_i}$, where index i labels the quark in the diagram.

Using the preceding expressions for the gluon and the quark propagators, the amplitude M_{fi} can be written as:

$$M_{fi} = -\frac{m_e}{E_e V}\frac{2^6}{3^2 s^3} g_s^2 e^2 \overline{v}(p_2)\gamma_\mu u(p_1) \int d^4q_a d^4q_b \frac{1}{\Delta_2\Delta_3\Delta_4\Delta_5}[TR]$$
$$\times \frac{N_v D_v(\hat{q_a})\phi_v(\hat{q_a})}{2\pi i}\frac{N_p D_p(\hat{q_b})\phi_p(\hat{q_b})}{2\pi i}. \tag{3.1.13}$$

Here [TR] is the trace over the gamma matrices appearing in the quark propagators in Eq.(3.1.8). Noting that the 4-dimensional volume element $d^4q = d^3\hat{q}Md\sigma$, we then perform contour integrations in the complex σ-plane by making use of the corresponding pole positions. The pole integrations over $dq_a^0 = M_a d\sigma_a$ and $dq_b^0 = M_b d\sigma_b$ in Eq.(3.1.13) can be expressed as: $\frac{1}{2\pi i}\int_{-\infty}^{\infty}\frac{M_a d\sigma_a}{\Delta_3\Delta_5} = \frac{1}{D(\hat{q_a})}$ and $\frac{1}{2\pi i}\int_{-\infty}^{\infty}\frac{M_b d\sigma_b}{\Delta_2\Delta_4} = \frac{1}{D(\hat{q_b})}$, where values of denominator functions $D(\hat{q}_a)$ and $D(\hat{q}_b)$ evaluated by contour integration in the complex σ- plane are expressible as in Eq.(2.3.41). After calculating the trace part in the above equation and employing the heavy quark approximation on relative momenta given in Eq.(3.1.12), one can obtain:

$$M_{fi} = -\frac{m_e}{E_e V}\frac{2^{14}\pi^2\alpha_{em}\alpha_s m_c^3}{3^2 s^3}\epsilon_{\alpha\mu\lambda\sigma}\varepsilon_\alpha P_{b\lambda}P_{a\sigma}\int d^3\hat{q}_a d^3\hat{q}_b N_v N_p \phi_v(\hat{q}_a)\phi_p(\hat{q}_b)[\overline{v}(p_2)\gamma_\mu u(p_1)] \tag{3.1.14}$$

where $\alpha_{em} = \frac{e^2}{4\pi}$, while $\alpha_s = g_s^2/4\pi$ and is given in Eq.(2.3.50). Let's define $\xi_a = \int d^3\hat{q}_a N_v \phi_v(\hat{q}_a)$ and $\xi_b = \int d^3\hat{q}_b N_p \phi_p(\hat{q}_b)$, which are values of wave functions at origins of J/ψ and η_c respectively.

Thus we can express the amplitude M_{fi} as,

$$M_{fi} = -\frac{m_e}{E_e V}\frac{2^{14}\pi^2\alpha_{em}\alpha_s m_c^3}{3^2 s^3}\epsilon_{\alpha\mu\lambda\sigma}\varepsilon_\alpha P_{b\lambda}P_{a\sigma}[\overline{v}(p_2)\gamma_\mu u(p_1)]\xi_a\xi_b. \tag{3.1.15}$$

Here N_p and N_v in $\xi_{a,b}$ are the BS normalizers for η_c and J/ψ respectively which are evaluated from Eq.(2.4.63) and Eq.(2.4.67).

The values of BS normalizers thus obtained for J/ψ and η mesons are $N_v = .0504 GeV^{-3}$ and $N_P = .0410 GeV^{-3}$ respectively.

The total amplitude for the process $e^+e^- \longrightarrow J/\Psi\eta_c$ can be obtained by summing over the amplitudes of all the four diagrams shown in Fig.3.1. For that matter the amplitude obtained from the first diagram is the same as the amplitude from each of the remaining three diagrams in Fig.3.1. Thus, the total amplitude is 4 times the amplitude from the first diagram. The unpolarized total cross section is obtained by summing over various J/Ψ spin-states and averaging over those of the initial state e^+e^-. To calculate the cross section, we need to calculate the total average probability per unit time, $\frac{|\overline{s_{fi}}|^2}{T}$ and then the differential cross section is given by

$$d\sigma = \frac{\frac{|\overline{s_{fi}}_{tot}|^2}{T}}{|\overrightarrow{J}_{in}|}\frac{d^3\overrightarrow{P}_a}{(2\pi)^3 2E_a}\frac{d^3\overrightarrow{P}_b}{(2\pi)^3 2E_b}, \tag{3.1.16}$$

where $|\overrightarrow{J}_{in}|$ is the current density which is given by

$$|\overrightarrow{J}_{in}| = \frac{1}{V}|\frac{\overrightarrow{p}_1}{E_1} - \frac{\overrightarrow{p}_2}{E_2}|. \tag{3.1.17}$$

In covariant form $|\overrightarrow{J}_{in}|$ can be expressed by

$$E_1E_2|\overrightarrow{J}_{in}| = \frac{1}{V}\sqrt{(p_1.p_2)^2 - (m_1m_2)^2}. \tag{3.1.18}$$

The total average probability per unit time, $\frac{|\overline{s_{fi}}|^2}{T}$ is obtained from the scattering amplitude. That means probability is given by

$$|s_{tot}|^2 = |M_{tot}|^2[(2\pi)^4\delta^4(p_1 + p_2 - P_a - P_b)]^2. \tag{3.1.19}$$

The square of the Dirac delta function in the above equation can be written as

$$[(2\pi)^4\delta^4(p_1 + p_2 - P_a - P_b)]^2 = (2\pi)^4VT\delta^4(p_1 + p_2 - P_a - P_b). \tag{3.1.20}$$

Thus, the total average probability per unit time is the sum over the final spin states and average over the initial spin states and is given by

$$\frac{\overline{|s_{tot}|}^2}{T} = \frac{1}{4}\sum_{s_1=1}^{2}\sum_{s_2=1}^{2}\sum_{s'=1}^{3}\overline{|M_{tot}|}^2[(2\pi)^4\delta^4(p_1 + p_2 - P_a - P_b). \tag{3.1.21}$$

Therefore, the differential cross section will be

$$d\sigma = VE_1E_2\frac{\frac{\overline{|s_{tot}|}^2}{T}}{\sqrt{(p_1.p_2)^2 - (m_1m_2)^2}}\frac{d^3\overrightarrow{P}_a}{(2\pi)^3 2E_a}\frac{d^3\overrightarrow{P}_b}{(2\pi)^3 2E_b}. \tag{3.1.22}$$

To obtain the total cross section, we need to know the value of the scattering matrix element, M_{fi}. This is because when we perform the integrations over $d^3\overrightarrow{P_a}$ and $d^3\overrightarrow{P_b}$, M_{fi} is a function $\overrightarrow{P_a}$, and $\overrightarrow{P_b}$.

Calculation of $|M_{tot}|^2$

The total scattering matrix is the sum of the contributions by each of the four Feynman diagrams but each diagrams contribute equally. Therefore, the total scattering matrix element is 4 times the contribution from the first Feynman diagram. Thus,

$$M_{tot} = -\frac{m_e}{E_e V}\frac{2^{16}\pi^2\alpha_{em}\alpha_s m_c^3}{3^2 s^3}\epsilon_{\alpha\mu\lambda\sigma}\varepsilon_\alpha P_{b\lambda}P_{a\sigma}[\overline{v}(p_2)\gamma_\mu u(p_1)]\xi_a\xi_b, \tag{3.1.23}$$

$$|M_{tot}|^2 = M_{tot}M_{tot}^\dagger, \tag{3.1.24}$$

where $M_{tot}^\dagger$ is given by

$$M_{tot}^\dagger = -\frac{m_e}{E_e V}\frac{2^{16}\pi^2\alpha_{em}\alpha_s m_c^3}{3^2 s^3}\epsilon_{\alpha'\mu'\lambda'\sigma'}\varepsilon_{\alpha'}^* P_{b\lambda'}P_{a\sigma'}[\overline{v}(p_2)\gamma_\nu u(p_1)]^\dagger\xi_a\xi_b, \tag{3.1.25}$$

and

$$[\overline{v}(p_2)\gamma_\nu u(p_1)]^\dagger = -[\overline{u}(p_1)\gamma_\nu v(p_2)]. \tag{3.1.26}$$

In order to find $|M_{tot}|^2$, we need to average it by taking sum over the final spin states and average over the initial spin states and hence the average of $|M_{tot}|^2$ is given by

$$\overline{|M_{tot}|^2} = \frac{1}{4}\sum_{sum}|M_{tot}|^2. \tag{3.1.27}$$

Using[31]

$$\begin{aligned}
\sum_{s_1=1}^{2} u_1^{(s_1)}(\overrightarrow{p}_1)\overline{u}_1^{(s_1)}(\overrightarrow{p}_1) &= \frac{-i\gamma.p_1 + m_e}{2m_e},\\
\sum_{s_2=1}^{2} v_2^{(s_2)}(\overrightarrow{p}_2)\overline{v}_2^{(s_2)}(\overrightarrow{p}_2) &= -\frac{i\gamma.p_2 + m_e}{2m_e},\\
\sum_{s'=1}^{3} \epsilon_\alpha\epsilon_{\alpha'}^* &= \delta_{\alpha\alpha'} - \frac{P_\alpha P_{\alpha'}}{P^2},
\end{aligned} \tag{3.1.28}$$

one can obtain

$$\overline{|M_{tot}|^2} = \frac{1}{16}\frac{2^{32}\pi^4\alpha_{em}^2\alpha_s^2 m_c^6}{3^4 s^6 E_e^2 V^2}\xi_a^2\xi_b^2 H_{\mu\mu'}L_{\mu\mu'}, \tag{3.1.29}$$

where $H_{\mu\mu'}$ is the hadronic tensor which is given by

$$H_{\mu\mu'} = \epsilon_{\alpha\mu\lambda\sigma}\epsilon_{\alpha\mu'\lambda'\sigma'}P_{b\lambda}P_{a\sigma}P_{b\lambda'}P_{a\sigma'}, \tag{3.1.30}$$

which is also expressible as

$$H_{\mu\mu'} = \delta_{\mu\mu'}(P_a^2 P_b^2 - (P_a.P_b)^2) - P_{a\mu}(P_{b\mu'}P_b^2 - P_a.P_b P_{b\mu'}) + P_{b\mu}(P_{a\mu'}P_a.P_b - P_a^2 P_{b\mu'}), \tag{3.1.31}$$

and $L_{\mu\mu'}$ is the leptonic tensor which is given by

$$L_{\mu\mu'} = 4[p_{1\mu}p_{2\mu'} - \delta_{\mu\nu}p_1.p_2 + p_{1\mu'}p_{2\mu}]. \tag{3.1.32}$$

Thus, substituting Eq.(3.1.32) and Eq.(3.1.31) into Eq.(3.1.29) and after some mathematical calculation, one can get for the total cross section σ which is given by

$$\sigma = \frac{4m_e^2}{32\pi}\frac{\sqrt{s-16m_c^2}}{s^{\frac{3}{2}}}\int \frac{1}{4}\sum_{spin}\overline{\mid M_{tot}\mid}^2 dcos\theta \tag{3.1.33}$$

where the masses of the leptons are ignored in the calculation. Explicitly $\overline{\mid M_{tot}\mid}^2$ is given by

$$\frac{1}{4}\sum_{spin}\mid M_{tot}\mid^2 = \frac{2^{30}\pi^4\alpha_{em}^2\alpha_s^2 m_c^6}{3^4 s^5 4m_e^2}(-32m_c^4 + t^2 + u^2)\xi_a^2\xi_b^2 \tag{3.1.34}$$

where $t = -(p_1 - P_a)^2$ and $u = -(p_1 - P_b)^2$ are the Mandelstam's variables. Therefore, in the CM frame, the total cross section is given by:

$$\sigma = \frac{2^{30}\pi^3\alpha_{em}^2\alpha_s^2 m_c^6}{83^5 s^4}(1 - \frac{16m_c^2}{s})^{\frac{3}{2}}\xi_a^2\xi_b^2 \tag{3.1.35}$$

3.2 Numerical Results:

The basic input parameters in the calculation are just four: $C_0 = 0.29$, $\omega_0 = 0.158 GeV$, QCD length scale, $\Lambda_{QCD} = 0.200 GeV$, and the charmed quark mass, $m_c = 1.530 GeV$ [19,23]. The numerical values of inverse range parameter β calculated from Eq.(2.3.52) are $\beta_{J/\psi} = .4989 GeV$ and $\beta_{\eta_c} = .4388 GeV$. To calculate the values of β, for the two hadrons, the experimental hadron masses are taken as, $M_{J/\psi} = 3.096 GeV$ and $M_{\eta_c} = 2.982 GeV$. With these parameters the total cross section for the above process at $\sqrt{s} = 10.6 GeV$ is calculated to be $\sigma = 21.75 fb$.

3.3 Discussion

In this section we have calculated the cross section of the exclusive process of $e^+e^- \longrightarrow J/\Psi\eta_c$ at energy $\sqrt{s} = 10.6 GeV$ in the framework of BSE under CIA[20,21,32] using only the leading order (LO) diagrams in QCD. We find the theoretical value of $\sigma[e^+e^- \longrightarrow J/\Psi\eta_c] = 21.75 fb$[33], which is broadly in agreement with the Babar's data $\sigma[e^+e^- \longrightarrow J/\Psi\eta_c] = (17.6 \pm 2.8 \pm 2.1) fb$ [24] and the Belle's data, $\sigma[e^+e^- \longrightarrow J/\Psi\eta_c] = (25.6 \pm 2.8 \pm 3.4) fb$ [25,26].

It had been noticed earlier that NRQCD predictions [34,35] for the above process at $\sqrt{s} = 10.6 GeV$ using leading order diagrams alone give cross sections which are much less than data[24,25,26]. Such a large discrepancy between experimental results and theoretical predictions has been a challenge to the understanding of charmonium production through NRQCD. Many studies were performed to resolve this problem. For instance Braaten and Lee[27] first showed that results on cross section are found to improve considerably when relativistic corrections are incorporated. Then it was found that to obtain cross sections from NRQCD which are consistent with data, one has to incorporate NLO QCD corrections [28,29]. However in these studies it was found that the value of total NLO contribution to cross section is nearly twice the LO contribution. In the present calculations under the relativistic framework of BSE under CIA, we obtained results for cross sections which are in good agreement with data [24,25,26] using leading order QCD processes alone though we have employed the heavy quark approximation ($q << M$ and $P \sim M$) on the quark and gluon propagators on lines of [36]. However we have not made use of the non-covariant heavy quark limit as in Eq.(3-4) of Ref.[36] and work with the exact propagators of the quarks constituting the two hadrons. This is a validation of the fact that BSE which is firmly rooted in field theory and which incorporates relativistic effects within its premises is ideally suited to describe not only low energy processes, but even processes at high energies such as high energy hadronic scattering and production processes.

The approach in this thesis is quite different from the approach in Ref.[36] in the sense that we employ the framework of BSE under CIA which is a relativistic generalization of Instantaneous Approximation (IA). Further, to calculate their results, Ref.[36] has made use of heavy quark limit on the propagators of all the heavy quarks and anti-quarks, where the propagators have been simplified as in their Eq.(3) and (4) which in fact is non-covariant. Also to simplify their calculation of amplitude in their Eq.(22), [36] makes use of the heavy quark approximation, in that the propagators of quark and gluon are independent of relative momenta q_a and q_b of the two hadrons since the masses of quarks are large compared to their relative momentum. However in this thesis, we only make use of the above heavy quark approximation ($q << M$ and $P \sim M$) only in the sense of simplifying the integrals for amplitude calculation as done in [36], but we do not employ the non-covariant heavy quark limit on the quark and anti quark propagators and instead work with the full quark and anti-quark propagators for the quarks constituting the hadrons. In doing so using CIA, we also see that our results on $\sum_s |M_{tot}|^2$ in Eq.(3.1.34) and cross section in Eq.(3.1.35) of our thesis are not exactly similar to results of[36]. In this regard, we wish to point out that our amplitude and cross sectional formulae involve the 4D BS normalizers N_V and N_P which are calculated in the framework of CIA and whose numerical values are explicitly worked out for both the hadrons, J/ψ and η_c as $N_v = .0504GeV^{-3}$ and $N_P = .0410GeV^{-3}$ respectively. These normalizers enter the amplitude and cross sectional formulae through the definitions of values of wave functionsξ_a and ξ_b of the two hadrons at their origins, which is not so in case of Ref.[36]. Further, the input BSE kernel and hence the input parameters employed by us and by Ref.[36] are completely different. While we employ "vector" confinement, ie. we make use of a common form $(\gamma_\mu^{(1)}\gamma_\mu^{(2)})$ for both one-gluon exchange as well as confining terms in the kernel as in Eq.(2.3.50) (for details see references [17–21]) , Ref.[36] employs a scalar $(1^{(1)}.1^{(1)})$ form for confinement, while vector form $(\gamma_\mu^{(1)}\gamma_\mu^{(2)})$ for one-gluon exchange. Further the scalar form of confining potential in [36]is also different from our case. Whereas Ref.[36]uses linear confinement $(\sim r)$ which is true in case of heavy quark (c,b) systems, we have used a general form of confinement potential in Eq.(2.3.50) which simulates the effect of linear confinement $(\sim r)$ for heavy quark sector (large m_1, m_2) while retaining harmonic form $(\sim r^2)$ for light quark sector (small m_1, m_2) . As far as the numerical results on cross section in this thesis and Ref.[36] are concerned, they are quite close. This may be due to the fact that for systems comprising of heavy quarks (c,b), the CIA results may lead to IA results when heavy quark approximation is imposed. However this may not be so for systems comprising of light quarks (u,d,s).

However in the present calculation, we used only the first of the leading order(LO) Dirac covariants (γ_5 and $i\gamma.\varepsilon$)in hadron-vertex functions for J/ψ and η_c mesons respectively. They were identified as most leading covariants in accordance with our power counting scheme. These covariants give maximum contribution to calculation of meson observables such as decay constants etc. It can also be seen here that the results on cross section for the process $e^+e^- \longrightarrow J/\Psi + \eta_c$ employing these most leading of the LO covariants brings theoretical results close to data [30,31,32]. We now also intend to see the effect of incorporation of both LO and the NLO Dirac covariants (to the vertex functions of these mesons) on cross section for the process studied. The contribution from NLO covariants is expected to be much lesser than the contribution from LO covariants in line with the recent studies on meson decays[19,20,21]. And this is more so for heavy mesons comprising of c and b quarks. It is expected that the results of cross section will improve further with incorporation of both LO and NLO covariants and without employing the heavy quark approximation on the quark and gluon propagators. This calculation will be quite rigorous.

Chapter 4

Low energy application of BSE under CIA

4.1 Radiative decays of light equal mass mesons through the process $h \rightarrow h' + \gamma$

In this section we study the radiative decays of equal mass vector mesons through the process, $h \rightarrow h'\gamma$ taking h and h' as equal mass vector and pseudoscalar mesons respectively. This process has been studied in the framework of Bethe-Salpeter Equation (BSE) under Covariant Instantaneous Ansatz (CIA).

4.1.1 EM transition amplitude

In lowest order, the Feynman diagrams for the process: $h \rightarrow \gamma h^{'}$ are shown in figure below, where h is the vector meson in the initial state and $h^{'}$ is the pseudoscalar meson in the final state.

The scattering amplitude for this process for Fig.(4.1a) is given by

$$s_{fi} = (2\pi)^4 M_a \delta^4(P - P' - k), \tag{4.1.1}$$

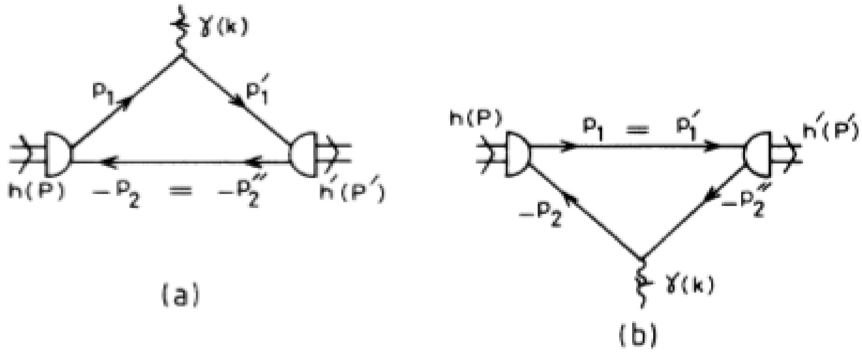

Figure 4.1: Electromagnetic transition amplitudes for the process: $h \to \gamma h^{'}$ via the quark triangle loop diagrams.

where the electromagnetic transition amplitude for Fig.(4.1a) is,

$$M_a = \frac{1}{\sqrt{2\omega_k V}} \int d^4q \mathrm{Tr}[\overline{\Psi}(P', q')(-ie_Q\gamma \cdot \epsilon_\gamma^*)\Psi(P, q)(i\gamma \cdot p_2 + m_2)] \tag{4.1.2}$$

where $\overline{\psi}(P', q')$ is the adjoint 4D BS wave function for pseudoscalar meson, while $\psi(P, q)$ is the 4D wave function for vector meson. e_Q is the electrical charge of quark No.1 with which the photon couples. ϵ_γ^* is the polarization vector of the photon. Inserting the forms of 4D BS wave functions and the corresponding Hadron-quark vertex functions from Eq.(2.3.45-2.3.48) in Eq.(4.1.2), one can write the above amplitude corresponding to the first triangle diagram, Fig.(4.1a) as,

$$M_a = \frac{1}{\sqrt{2\omega_k V}} \int d^4q$$
$$\times \mathrm{Tr}[S_F(-p_2)\Gamma^p(\widehat{q'})S_F(p_1^{'})(-ie_Q\gamma \cdot \epsilon_\gamma^*)S_F(p_1)\Gamma^V(\widehat{q})S_F(-p_2)(i\gamma \cdot p_2 + m_2)] \tag{4.1.3}$$

This can in turn be written as,

$$M_a = (-ie_Q)\frac{1}{\sqrt{2\omega_k V}}\frac{1}{(2\pi i)^2}N_pN_V \int \frac{D_p(\widehat{q'})D_V(\widehat{q})\phi_p(\widehat{q'})\phi_V(\widehat{q})}{\Delta_1\Delta_2\Delta_1'}d^4q[\mathrm{TR}] \tag{4.1.4}$$

where the trace part over the product of Gamma matrices, [TR] is expressed as:

$$[\mathrm{TR}] = \mathrm{Tr}[(i\gamma\cdot p_2+m)\gamma_5(-i\gamma\cdot p_1^{'}+m)\gamma\cdot\varepsilon_\gamma^*(-i\gamma\cdot p_1+m)\gamma\cdot\varepsilon_h] = -4m\epsilon_{\mu\nu\lambda\beta}P_\mu^{'}\varepsilon_{\gamma\nu}^*P_\lambda\varepsilon_{h\beta}. \tag{4.1.5}$$

Here ε_h is the polarization vector of the vector meson. Similarly, the amplitude, M_b corresponding to the process in Fig.(4.1b)is equal to the amplitude corresponding to Fig.(4.1a), except for the value of e_Q which will be the electric charge of quark No. 2 with which the photon couples to in Fig.(4.1b). The total amplitude for the process: $h \to h'\gamma$ is given by $M_{tot} = M_a + M_b$. For the ρ and ω mesons which involve the lightest u, d quarks, the total amplitude can be conveniently expressed as,

$$\begin{aligned} M_{tot} &= \frac{4me}{\sqrt{2\omega_k V}4\pi^2}N_pN_V\epsilon_{\mu\nu\lambda\beta}P_\mu^{'}\varepsilon_{\gamma\nu}^*P_\lambda\varepsilon_{h\beta}[\chi], \\ \chi &= \int\frac{D_p(\widehat{q'})D_V(\widehat{q})\phi_p(\widehat{q'})\phi_V(\widehat{q})}{\Delta_1\Delta_2\Delta_1'}d^4q \end{aligned} \tag{4.1.6}$$

where $e_u = \frac{2}{3}e$ and $e_d = -\frac{1}{3}e$ are taken as the electric charges of u and d-quarks respectively. And χ is the 4D integral over the poles of all the quark propagators involved in the process. In the expression for M_{tot}, N_V and N_P are the 4D BS normalizers for vector and pseudoscalar mesons respectively which are evaluated from Eq.(2.4.63) and Eq.(2.4.67).

The numerical values of BS normalizers for $\rho^\pm$, ω and $\pi^{0,\pm}$ mesons so obtained are listed in the section on Numerical Calculations.

4.1.2 Calculation of the 4D integral, χ

The evaluation of this 4D integral in Eq.(4.1.6) over the poles of the quark propagators is one of the most difficult tasks of this work. In the expression χ, the denominator functions for vector and pseudoscalar mesons are given respectively as:

$$D_V(\widehat{q}) = \frac{1}{2\pi i}\int_{-\infty}^{\infty}\frac{M d\sigma}{\Delta_1\Delta_2}, D_p(\widehat{q'}) = \frac{1}{2\pi i}\int_{-\infty}^{\infty}\frac{M' d\sigma'}{\Delta_2\Delta_1'}. \tag{4.1.7}$$

From conservation of 4 momenta, we have $P = P' + k, p_1 = p_1' + k$, where $P = p_1 + p_2$. We then express the individual quark momenta $p_{1,2}$, p_1', $\Delta_{1,2}$ and Δ_1' in terms of total hadron momenta, P, P' and internal hadron momenta, q, q' as:

$$\begin{aligned}
&p_1 = \frac{P}{2} + q,\\
&p_2 = \frac{P}{2} - q = \frac{P'}{2} - q',\\
&p_1' = \frac{P'}{2} + q',\\
&\Delta_1 = p_1^2 + m^2 = -M^2(\sigma + \frac{1}{2})^2 + \omega^2,\\
&\omega^2 = \widehat{q}^2 + m^2,\\
&\Delta_2 = p_2^2 + m^2 = -M^2(\sigma - \frac{1}{2})^2 + \omega^2.
\end{aligned} \tag{4.1.8}$$

Since in Fig.4.1a $p_2 = p"_2$, we can also express Δ_2 as,

$$\begin{aligned}
&\Delta_2 = p"^2_2 + m^2 = -M'^2(\sigma' - \frac{1}{2})^2 + \omega'^2,\\
&\omega'^2 = \widehat{q'}^2 + m^2,
\end{aligned} \tag{4.1.9}$$

and Δ_1' as,

$$\Delta_1' = p_1'^2 + m^2 = -M'^2(\sigma' + \frac{1}{2})^2 + \omega'^2. \tag{4.1.10}$$

From conservation of 4 momenta , we can express the momentum of the emitted photon as, $k = P - P'$. And from the relation $p_2 = \frac{P}{2} - q = \frac{P'}{2} - q'$ one can obtain a relation for q' in terms of the independent variable q as,

$$q' = -\frac{k}{2} + q. \tag{4.1.11}$$

In the rest frame of the initial meson, we can express, $P = (0, iM), P' = (\overrightarrow{P}', iE'), k = (\overrightarrow{k}, i\omega_k) = (-\overrightarrow{P}', i\omega_k), q = (\widehat{q}, iM\sigma)$,and $q' = (\widehat{q}', iM'\sigma')$.

Also,

$$P \cdot q' = -\frac{k \cdot P}{2} + P \cdot q. \tag{4.1.12}$$

We can further express,the scalar products of momenta $P \cdot q' = -MM'\sigma'$ and $P \cdot q = -M^2\sigma$. Similarly, we can obtain a relationship between the time like momentum component σ' of pseudoscalar meson in terms of the time like momentum component σ of vector meson as

$$\sigma' = \frac{M}{M'}(\sigma - \frac{1}{4}) + \frac{M'}{4M}. \tag{4.1.13}$$

We can also define the dependent variables ω', and q' in terms of the independent variables σ, ω and q by making use of the expression for Δ_2 for quark No. 2 as,

$$\Delta_2 = -M^2(\sigma - \frac{1}{2})^2 + \omega^2 = -M'^2(\sigma' - \frac{1}{2})^2 + \omega'^2. \tag{4.1.14}$$

The above equation leads to the relationship between ω' and ω as

$$\omega'^2 = \omega^2 + \frac{M^2}{2}(1 - \frac{M'}{M})^2(\sigma - \frac{1}{2}) + \frac{M^2}{16}(1 - \frac{M'}{M})^4, \tag{4.1.15}$$

and which implies that for equal mass meson case considered here (where, $\omega^2 = m^2 + \widehat{q}^2$ and $\omega'^2 = m^2 + \widehat{q}'^2$), we get the relationship between square of the transverse component $\widehat{q}^2$ of internal momentum of vector meson with the square of the transverse component $\widehat{q}'^2$ of internal momentum of pseudoscalar meson as,

$$\widehat{q'}^2 = \widehat{q}^2 + \frac{M^2}{2}(1 - \frac{M'}{M})^2(\sigma - \frac{1}{2}) + \frac{M^2}{16}(1 - \frac{M'}{M})^4. \tag{4.1.16}$$

The appearance of time like momentum components σ of vector meson in the expression for square of the effective 3D momentum vector, $\widehat{q'}^2$ for pseudoscalar meson can be noticed in the above equation. We can also define Δ_1' in terms of the independent variables σ, and ω, which after some steps can be expressed as,

$$\Delta_1' = -M^2(\sigma - \frac{1}{2} + \frac{M'}{M})^2 - \frac{\omega f}{M^2}, \tag{4.1.17}$$

where

$$f = 1 - \frac{MM'}{2\omega^2}(1 - \frac{M'}{M})^2. \tag{4.1.18}$$

Finally, we can also express the 3D ground state wave function for pseudoscalar meson, $\phi_P(\widehat{q'})$ as

$$\phi_P(\widehat{q'}) = e^{-\frac{\widehat{q}^2}{2\beta'^2}}.e^{-\frac{M^2}{4\beta'^2}(1-\frac{M'}{M})^2(\sigma-\frac{1}{2})}.e^{-\frac{M^2}{32\beta'^2}(1-\frac{M'}{M})^4}. \tag{4.1.19}$$

As seen from Eq.(4.1.16), the square of the effective 3D vector for pseudoscalar meson $\widehat{q'}^2$ involves not only the square of the effective 3D vector for vector meson, $\widehat{q}^2$, but also the mixing from the time like momentum components σ of the vector meson. This is what leads to appearance of time-like momentum components in the gaussian factors associated with the vertex function of pseudoscalar meson as pointed out earlier in reference [17] and is the root cause of complexity in the calculations of transition amplitudes for such processes involving triangle loop diagrams like the above. We now try to show how to handle such problems and calculate meaningful results. We can decompose the 3D wave function for pseudoscalar meson, $\phi_P(\widehat{q'})$ in above equation as,

$$\begin{aligned}
\phi_P(\widehat{q'}) &= K\phi_P(\widehat{q})\phi_P(\sigma), \\
\phi_P(\widehat{q}) &\equiv e^{-\frac{\widehat{q}^2}{2\beta'^2}}, \\
\phi_P(\sigma) &\equiv e^{-\frac{M^2}{4\beta'^2}(1-\frac{M'}{M})^2(\sigma-\frac{1}{2})}, \\
K &\equiv e^{-\frac{M^2}{32\beta'^2}(1-\frac{M'}{M})^4}.
\end{aligned} \tag{4.1.20}$$

Thus we note that the effective 3D BS wave function $\phi_P(\widehat{q'})$ which enters in the expression for the 4D integral χ in Eq.(4.1.6) is completely expressible in terms of independent variables, $\widehat{q}$ and σ. In the integral χ, there are Denominator functions $D_P(\widehat{q'})$ for pseudoscalar meson and $D_V(\widehat{q})$ for vector meson which are to be evaluated. $D_V(\widehat{q})$ is a function of the independent variable, $\widehat{q}$ and is easily calculated in its rest frame by the usual procedure of evaluating the contour integral,

$$D_V(\widehat{q}) = \frac{1}{2\pi i}\int_{-\infty}^{\infty}\frac{Md\sigma}{\Delta_1\Delta_2} \tag{4.1.21}$$

by noting the pole positions of the poles of Δ_1 and Δ_2 which occur at:

$$\begin{aligned}\Delta_1 = 0 \Rightarrow \sigma_1^{\pm} &= \pm\frac{\omega}{M} - \frac{1}{2} \mp i\varepsilon,\\ \Delta_2 = 0 \Rightarrow \sigma_2^{\pm} &= \pm\frac{\omega}{M} + \frac{1}{2} \mp i\varepsilon\end{aligned} \tag{4.1.22}$$

and can be worked out as:

$$D_V(\widehat{q}) = \omega(4\omega^2 - M^2). \tag{4.1.23}$$

However, the expression for denominator function for pseudoscalar meson, $D_P(\widehat{q'})$ is quite complicated. And further we need to express it in terms of the independent variable $\widehat{q}$. To calculate it, we start with its definition as,

$$D_p(\widehat{q'}) = \frac{1}{2\pi i}\int_{-\infty}^{\infty}\frac{M' d\sigma'}{\Delta_2\Delta_1'}. \tag{4.1.24}$$

Here $d\sigma' = \frac{M}{M'}d\sigma$ from Eq.(4.1.13). Now to carry out integration over $d\sigma$, we note that σ integration poles occur at

$$\begin{aligned}\Delta_2 = 0 \Rightarrow \sigma_2^{\pm} &= \pm\frac{\omega}{M} + \frac{1}{2} \mp i\varepsilon,\\ \Delta_1' = 0 \Rightarrow \sigma_1^{\pm} &= \pm\frac{\omega}{M}\sqrt{1 - \frac{M^2x(1-x)^2}{2\omega^2}} + \frac{1}{2} \mp i\varepsilon\end{aligned} \tag{4.1.25}$$

(where Eq.(4.1.17) is used for Δ_1'). If the semi-circular contour is closed from below the Re(σ)- axis, residues from σ_2^+ and σ_1^+ poles will contribute to the integral. However if the contour is closed from above the Re(σ)- axis, the residues from σ_2^- and σ_1^- poles will contribute to the integral. The results of σ- integration in Eq.(4.1.24) where the contour can be closed either from above or from below the Re(σ)- axis yields the expression for $D_P(\widehat{q'})$ as,

$$D_p(\widehat{q'}) = \frac{2\omega f[(1+f)^2\omega^2 - x^2M^2]}{1+f},$$
$$x = \frac{M'}{M},$$
$$f = 1 - \frac{M^2x}{2\omega^2}(1-x)^2. \tag{4.1.26}$$

Thus we have been able to successfully express $D_P(\widehat{q'})$ in terms of the independent variable $\widehat{q}$ along with $\phi_P(\widehat{q'})$ done earlier. Now we try to evaluate the 4D integral χ in Eq.(4.1.6). We can also simplify $\frac{1}{\Delta_1\Delta_2\Delta_1'}$ in the integral χ as

$$\frac{1}{\Delta_1\Delta_2\Delta_1'} = \frac{1}{\omega_k Mx}[\frac{1}{\Delta_1\Delta_2} - \frac{x}{\Delta_2\Delta_1'} - \frac{1-x}{\Delta_1\Delta_1'}] \tag{4.1.27}$$

where $\omega_k = \frac{M^2-M'^2}{2M}$. Therefore one can express χ as

$$\chi = \frac{1}{\omega_k Mx}\int d^4q D_V(\widehat{q})D_P(\widehat{q'})\phi_V(\widehat{q})\phi_P(\widehat{q'})[\frac{1}{\Delta_1\Delta_2} - \frac{x}{\Delta_2\Delta_1'} - \frac{1-x}{\Delta_1\Delta_3}]. \tag{4.1.28}$$

Putting $\phi_P(\widehat{q'})$ from Eq.(4.1.19) into the above equation, we can express χ as,

$$\chi = \frac{K}{\omega_k Mx}\int d^3\widehat{q}D_V(\widehat{q})D_P(\widehat{q'})\phi_V(\widehat{q})\phi_P(\widehat{q})\int_{-\infty}^{\infty}\phi_P(\sigma)[\frac{1}{\Delta_1\Delta_2} - \frac{x}{\Delta_2\Delta_1'} - \frac{1-x}{\Delta_1\Delta_1'}]Md\sigma \tag{4.1.29}$$

where the quantities $K, \phi_P(\widehat{q})$ and $\phi_P(\sigma)$ are defined in Eq.(4.1.20). Thus we can express χ as,

$$\chi = \frac{K}{\omega_k Mx}\int d^3\widehat{q}D_V(\widehat{q})D_P(\widehat{q'})\phi_V(\widehat{q})\phi_P(\widehat{q})(\chi_1+\chi_2+\chi_3) \tag{4.1.30}$$

where

$$\chi_1 = \int_{-\infty}^{\infty} \frac{\phi_P(\sigma) M d\sigma}{\Delta_1 \Delta_2}, \tag{4.1.31}$$

$$\chi_2 = -x \int_{-\infty}^{\infty} \frac{\phi_P(\sigma) M d\sigma}{\Delta_2 \Delta_1'}, \tag{4.1.32}$$

and

$$\chi_3 = -(1-x) \int_{-\infty}^{\infty} \frac{\phi_P(\sigma) M d\sigma}{\Delta_1 \Delta_1'}. \tag{4.1.33}$$

We note the pole positions for σ integration for $\Delta_1, \Delta_2, \Delta_1'$ in the above integrals from Eqs.(4.1.22) and Eq.(4.1.25) above.

If the semi-circular contours in the 3 integrals above are closed from below the Re(σ)- axis, residues from σ_1^+, σ_2^+ and σ_1^+ poles will contribute to the above integrals. However if the contours are closed from above the $Re(\sigma)$- axis, the residues from σ_1^-, σ_2^- and σ_1^- poles will contribute to the above integrals. The results of σ- integration in above equations where the contour can be closed either from above or from below the Re(σ)- axis yields the analytic expressions for the integrals, χ_1, χ_2 and χ_3 as:

$$\chi_1 = -2\pi\{\frac{e^{[\frac{(1-x)^2 M^2 (1-\frac{\omega}{M})}{4\beta'^2}]}}{2M(M-2\omega)\omega} + \frac{e^{[\frac{-(1-x)^2 M\omega}{4\beta'^2}]}}{2M\omega(M+2\omega)}\}, \tag{4.1.34}$$

$$\chi_2 = x(2\pi)\{-\frac{e^{[\frac{-(1-x)^2 M\omega}{4\beta'^2}]}}{2\omega(-x^2M^2 - 2xM\omega - \omega^2 + f\omega^2)}$$
$$+\frac{e^{[\frac{(1-x)^2 M^2 (x-\frac{\sqrt{f}\omega}{M})}{4\beta'^2}]}}{2\sqrt{f}\omega(x^2M^2 - 2\sqrt{f}xM\omega - \omega^2 + f\omega^2)}\}, \tag{4.1.35}$$

$$\chi_3 = (1-x)2\pi\{\frac{e^{[\frac{(1-x)^2 M^2 (1-\frac{\omega}{M})}{4\beta'^2}]}}{2\omega(-M + xM + \omega + \sqrt{f}\omega)^2}\}. \tag{4.1.36}$$

These expressions for $\chi_{1,2,3}$ obtained above are put in Eq.(4.1.30) to finally obtain the numerical value for the 4-D integral, χ which will be employed for decay width calculation for various processes in the next section.

4.1.3 Decay width calculation

We can now come back to the decay width calculation. From Eq.(4.1.6) for total amplitude, M_{tot}, one can obtain

$$|\overline{M_{tot}}|^2 = \frac{m^2 M^4 \alpha_{em} N_p^2 N_V^2}{3\omega_k V \pi^3}(1-x^2)^2|\chi|^2. \tag{4.1.37}$$

To calculate the decay width, we need to know the average probability per unit time per unit volume and it is given by

$$\frac{|s_{tot}|^2}{VT} = (2\pi)^4 |M_{tot}|^2 \delta^4(P - P' - k), \tag{4.1.38}$$

and the decay width[37] is given by

$$d\Gamma = \frac{|s_{tot}|^2}{VT} 2M \frac{V d^3\overrightarrow{k}}{(2\pi)^3} \frac{d^3\overrightarrow{P'}}{(2\pi)^3 2E'}. \tag{4.1.39}$$

After performing the integration, one can obtain

$$\Gamma = \frac{|\overline{M_{tot}}|^2 V}{4\pi M^2}|\overrightarrow{P'}|^2, \tag{4.1.40}$$

where

$$|\overrightarrow{P'}|^2 = \omega_k = \tfrac{M^2 - M'^2}{2M}$$

and then the decay width for the process $h \to h'\gamma$ is given by

$$\Gamma_{h\to\gamma h'} = \frac{\alpha_{em} N_P^2 N_V^2 m^2 M^3}{24\pi^4}(1-x^2)^3|\chi|^2. \tag{4.1.41}$$

4.1.4 Numerical calculation

The input parameters employed in the calculation are: $C_0 = .29, \Lambda = .200$GeV, $\omega_0 = 0.158$GeV, $m_{u,d} = 0.265$GeV. Experimental meson masses are taken as: $M_{\pi^\pm} =$

.140GeV, $M_{\pi^0} = .135$GeV, $M_{\rho^\pm} = M_{\rho^0} = .770$GeV, $M_\omega = .782$GeV. The values of BS Normalizers are: $N_{\pi^0} = .599\mathrm{GeV}^{-3}$,$\mathrm{N}_{\pi^\pm} = .618\mathrm{GeV}^{-3}$,$\mathrm{N}_{\rho^\pm} = N_{\rho^0} = .359\mathrm{GeV}^{-3}$, $N_\omega = .347\ \mathrm{GeV}^{-3}$. The calculated values of the decay widths are given below[38] along with the corresponding central values of data in brackets as:

$$\Gamma(\rho^\pm \to \gamma\pi^\pm) = .959\times 10^{-4}\mathrm{GeV}(\mathrm{Expt.} = .671\times 10^{-4}\mathrm{GeV}^{(39)}))$$
$$\Gamma(\rho^0 \to \gamma\pi^0) = 1.110\times 10^{-4}\mathrm{GeV}(\mathrm{Expt.} = .894\times 10^{-4}\mathrm{GeV}^{(39)})$$
$$\Gamma(\omega^0 \to \gamma\pi^0) = 5.810\times 10^{-4}\mathrm{GeV}(\mathrm{Expt.} = 7.029\times 10^{-4}\mathrm{GeV}^{(39)}). \quad (4.1.42)$$

4.1.5 Discussion

In the first section of this chapter, we have employed Bethe-Salpeter framework under Covariant Instantaneous Ansatz (CIA) to calculate the radiative decay widths of equal mass vector mesons (ρ,ω) through the process $h \to h'\gamma$ using Feynman diagrams in lowest order. We have calculated the radiative decay widths for the processes: $\rho^\pm \to \gamma\pi^\pm$, $\rho^0 \to \gamma\pi^0$ and $\omega \to \gamma\pi^0$. The motivation for this work was our intention to resolve the problems involved in the calculations of triangle quark loop diagrams which appear in processes such as radiative meson decays, strong decays of hadrons etc. in BSE under CIA, which gives rise to extremely complex 4D loop integrals (as pointed out earlier in Ref.[17]) due to appearance of time like momentum components in gaussian factors associated with the vertex functions of the participating hadrons. In an effort to study such processes in BSE under CIA, we first try to highlight the above problem arising in radiative decays of equal mass vector mesons (ρ,ω), and then demonstrate a mathematical procedure which might lead to calculations of such processes involving triangle loop diagrams in CIA and calculate meaningful results.

In these processes involving quark triangle loop diagrams, it is to be noted that the square of the effective 3D vector for pseudoscalar meson $\widehat{q'}^2$ (Eq.4.1.16), involves not only the square of the effective 3D vector for vector meson, $\widehat{q}^2$, but also the mixing from the time like momentum components σ of the vector meson, and hence leading to the appearance of time-like (σ) momentum components in the gaussian factors in the 3D wave function, $\phi_P(\widehat{q'})$ associated with the vertex function $\Gamma^P(\widehat{q'})$ of pseudoscalar meson. This is the root cause of complexity in the calculations of transition amplitudes for such processes involving triangle loop diagrams like the above. In this work we have tried to show how to handle such problems and calculate meaningful results.

For instance, the calculation of 3D denominator function $D_P(\widehat{q'})$ for pseudoscalar meson (appearing in the expression for 4D integral, χ (Eq.(4.1.6) is itself an integral defined in Eq.(4.1.7) and is quite complex since it has to be expressed in terms of the independent variables σ and ω (or $\widehat{q}$). However one can derive the analytic expression for $D_P(\widehat{q'})$ in Eq.(4.1.7) by evaluating this contour integral so that $D_P(\widehat{q'})$ is a function of entirely of the independent variable, $\widehat{q}$. However, the calculation for the 3D denominator function $D_V(\widehat{q})$ for vector meson (which is in its rest frame in this process considered) is straight forward. The most significant problem which then remained was the calculation of the four dimensional integral, χ (defined in Eq.(4.1.6). This integral χ was handled once we defined each term in this integral in terms of independent variables, σ and $\widehat{q}$. The analytic integrations over $d\sigma$ in the complex σ-plane were performed so that χ was completely expressed in terms of a single independent variable,$\widehat{q}$ over which the numerical calculation were then carried out. This was done using Mathematica. The theoretically calculated values of the decay widths for the above processes are found to be in reasonable agreement with data[39].

Our results for decay widths in Eq.(4.1.41) can also be compared with results of some other calculations [40,41,42]. In a calculation under BSE framework [40], the decay widths calculated were: $\Gamma(\rho^\pm \to \gamma\pi^\pm) = .38 \times 10^{-4}$GeV, $\Gamma(\rho^0 \to \gamma\pi^0) = .38 \times 10^{-4}$GeV and $\Gamma(\omega \to \gamma\pi^0) = 3.35 \times 10^{-4}$GeV. In a recent calculation using Salpeter Equation based model [41,42], the results of radiative decay widths were: $\Gamma(\rho^\pm \to \gamma\pi^\pm) = .35 \times 10^{-4}$GeV, $\Gamma(\rho^0 \to \gamma\pi^0) = .35 \times 10^{-4}$GeV, and $\Gamma(\omega \to \gamma\pi^0) = 3.15 \times 10^{-4}$GeV. In another calculation using Salpeter equation by the same group but using a different form of confining potential[41,42], the results of decay widths were: $\Gamma(\rho^\pm \to \gamma\pi^\pm) = .21 \times 10^{-4}$GeV, $\Gamma(\rho^0 \to \gamma\pi^0) = .21 \times 10^{-4}$GeV and $\Gamma(\omega \to \gamma\pi^0) = 1.85 \times 10^{-4}$GeV. These results of other models are in broad agreement with our results in Eq.(4.1.41).

With this successful application of CIA framework to radiative decays of equal mass vector meson, we will also apply this framework to decays of other processes involving quark-triangle diagrams like strong decays of mesons ($h \to h'h$") in the next section as a test of this CIA dynamics.

4.2 Strong decays of vector mesons through the process $h \to h' + h''$

The strong decays of hadrons, ($h \to h' + h''$) have been of a considerable interest for any dynamical programme for hadrons. These hadronic transition amplitudes which involve quark triangle loops represent sensitive probes into the internal dynamics of

$q\overline{q}$ hadrons. These amplitudes are particularly convenient for testing finer details of any model for strong interaction dynamics and are evaluated through hadron-quark vertex functions $\Gamma(\widehat{q})$ operative at the three vertices. In this connection, we wish to mention that though a considerable amount of work has been done in decays of equal mass ground state vector mesons such as, $\rho \rightarrow \pi + \pi$, not much work has been done so far in decays of radially excited vector mesons such as $\omega(1420)$ and $\rho(1450)$ regarded as 1st radial $2S_1$ excitations of ω and ρ mesons. For some of the recent works on these mesons in various models, see Ref.[43–46]. It is seen that although there is general consensus on the existence of these states, there is considerable discrepancy on their decay widths. Also their experimental status is not very clear as can be seen from the recent PDG Tables[47], which shows a wide range of variation in data on their decay widths (eg. of $\omega(1420)$). Thus further investigations both in theory and experiment are required. The theoretical study of radially excited mesons is expected to provide us with a deeper understanding of internal structure of hadrons and of the effective inter-quark interactions. Towards this end, we study the strong decays of excited vector mesons, $\omega(1420)$ and $\rho(1450)$ through the process $h \rightarrow h' + h''$, taking h as radially excited equal mass vector meson, while h' and h" as equal mass ground state vector and pseudoscalar mesons respectively in the framework of Bethe-Salpeter Equation (BSE) under Covariant Instantaneous Ansatz (CIA) which has earlier given good predictions for electromagnetic decay constants of vector mesons through the process $V \rightarrow e^+ + e^-$[19], weak decay constants of unequal mass pseudoscalar mesons through the process $P \rightarrow l + \overline{\nu_l}$[20,21], two photon electromagnetic decays of equal mass pseudoscalar mesons through the process $P \rightarrow \gamma + \gamma$[21], radiative decays of equal mass vector mesons through the process,$h \rightarrow h' + \gamma$[38] as well as the recent high energy tests of this model in the study of double charmonium production in electron-positron annihilation at energies $\sqrt{s} = 10.6GeV$ through the process, $e^- + e^+ \rightarrow J/\psi + \eta_c$[33].

4.2.1 Transition amplitude for process $h \rightarrow h' + h''$

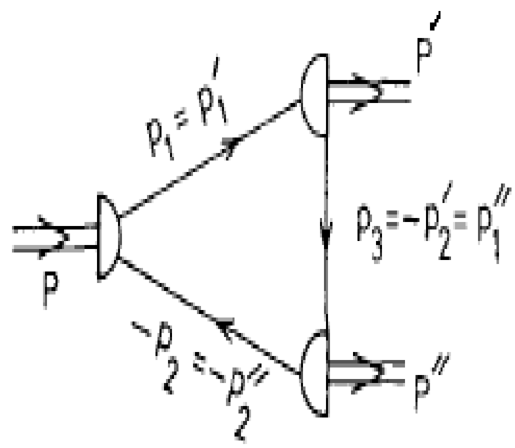

Figure 4.2: Leading order quark triangle diagram for $h \rightarrow h' + h''$. The other diagram is obtained by reversing the arrows of internal fermionic lines

The leading order quark-triangle diagram for the hadronic transition, $h \rightarrow h' + h''$ is shown in Fig.4.2, where the masses of hadrons are: (M, M' and M'') respectively with four momenta (P, P' and P''). The other diagram contributing to this process is the one with the directions of all internal fermion lines in the quark loop reversed. In this problem we will consider the two processes: $\omega(1420) \rightarrow \rho(770) + \pi(140)$ and $\rho(1450) \rightarrow \omega(782) + \pi(140)$. Here $\omega(1420)$ and $\rho(1450)$ are radially excited $2s_1$ states on which not much work has been done so far. There is considerable amount of discrepancy on their decay widths both as regards predictions of various models are concerned as well as experimental data. The labeling of quark momenta is[48]:

$$p_1 = p'_1,$$
$$p_3 = -p'_2 = p''_1,$$
$$-p_2 = -p''_2. \tag{4.2.43}$$

Due to the above equation, we can write the individual momenta of the three quarks in Fig. 4.2 as,

$$p_{1,2} = \frac{P}{2} \pm q,$$
$$p'_{1,2} = \frac{p'}{2} \pm q',$$
$$p''_{1,2} = \frac{P''}{2} \pm q''. \tag{4.2.44}$$

This ensure the overall momentum conservation, $P = P' + P''$ via the connections $P = p_1 + p_2$, $P' = p'_1 + p'_2$, and $P'' = p''_1 + p''_2$. The internal four-momenta of the hadrons are given by,

$$2q = p_1 - p_2,$$
$$2q' = p'_1 - p'_2,$$
$$2q'' = p''_1 - p''_2. \tag{4.2.45}$$

These give rise to relations:

$$q' = q + \frac{1}{2}P'',$$
$$q'' = q - \frac{1}{2}P'. \tag{4.2.46}$$

The scattering amplitude for the process $h \to h' + h''$ is given by:

$$S_{fi} = M_{fi}(2\pi)^4\delta^4(P' + P" - P), \tag{4.2.47}$$

where $M_{fi} \equiv M_{tot}$ is the total invariant amplitude, which is the sum of amplitudes for diagram in Fig.4.2 and a diagram where the directions of arrows of all internal fermionic lines are reversed. The contribution from the second diagram is the same as the diagram in Fig.4.2. Now, the invariant amplitude M_{fi} is,

$$M_{fi} = \sqrt{\frac{2}{3}}(2\pi)^8 \int d^4q Tr[\Gamma_h(\widehat{q}) s_F(p_1) \Gamma_{h'}(\widehat{q'}) s_F(p_3) \Gamma_{h"}(\widehat{q"}) s_F(-p_2)] \qquad (4.2.48)$$

with $\sqrt{\frac{2}{3}}$ being the color-isospin factor. Here, the color factor is $1/\sqrt{3}$, while the isospin factor is $\sqrt{2}$ (which involves a factor 2 coming from taking into account both the diagrams in Fig.4.2). It is further to be mentioned that this isospin factor which involves trace over the product of flavor matrices for all the three mesons h, h' and h'' is the same for both the processes, $\omega(1420) \to \rho\pi$ and $\rho(1450) \to \omega\pi$ on account of cyclic property of Trace. The 4D hadron-quark vertex function for ground state (1S) vector meson (h') in the final state of the process $h \to h' + h''$ as,

$$\Gamma_{h'}(\widehat{q'}) = i\gamma.\varepsilon' N_{h'} D_{h'}(\widehat{q'}) \phi_{h'}(\widehat{q'})/2\pi i, \qquad (4.2.49)$$

while the 4D hadron-quark vertex function for ground state (1S) pseudoscalar meson, h'' in the final state of the above process can be written as,

$$\Gamma_{h''}(\widehat{q''}) = \gamma_5 N_{h''} D_{h''}(\widehat{q''}) \phi_{h''}(\widehat{q''})/2\pi i. \qquad (4.2.50)$$

Here, $\phi_{h'}(\widehat{q'})$ and $\phi_{h''}(\widehat{q''})$ are the ground state 3D BS wave functions for vector meson, h', and pseudoscalar meson, h'' (with internal momenta q' and q'' respectively emitted in the final state of the above process), which satisfy the corresponding 3D BSE (on the surfaces $P'.q' = 0$ and $P''.q'' = 0$), which is appropriate for making contact with O(3)-like mass spectrum (for details see[17] and references therein), which is reducible to the equation for a 3D harmonic oscillator with coefficients depending on the mass M and total quantum number N. The ground state wave functions[17,19,21,46] deducible from this equation have gaussian structure and are expressed as:

$$\phi_{h'}(\widehat{q'}) = Exp[-\widehat{q}'^2/2\beta'^2],$$
$$\phi_{h''}(\widehat{q''}) = Exp[-\widehat{q}''^2/2\beta''^2], \quad (4.2.51)$$

while the 4D hadron-quark vertex function for 1st radially excited (2S) vector meson, h (with internal momentum q) is:

$$\Gamma_h(\widehat{q}) = i\gamma.\epsilon N_h D_h(\widehat{q})\phi_h(\widehat{q})/2\pi i \quad (4.2.52)$$

where the unnormalized 3D BS wave function $\phi_h(\widehat{q})$ for the 1st radially excited (2S) vector meson, h (which may be either, $\omega(1420)$ or $\rho(1450)$ depending on the process) in the harmonic oscillator basis used above can be easily guessed as:

$$\phi_h(\widehat{q}) = (-3\beta^2 + 2\widehat{q}^2)e^{-\widehat{q}^2/2\beta^2}, \quad (4.2.53)$$

(a similar form for 2S wave function in harmonic oscillator basis using variational arguments has been used in[49]. Here, β is the inverse range parameter which incorporates the content of BS dynamics and is dependent on the input kernel $K(q, q')$ (for details see[17,21,33]).

Plugging the forms of the hadron-vertex functions $\Gamma(\widehat{q})$ given in Eqs.(4.2.49,4.2.50) and Eq (4.2.52), for all the three mesons involved in this process, the quark propagators, $S_F(\pm p_i) = -i\frac{\mp i\gamma.p_i + m}{\Delta_i}$, $\Delta_i = p_i^2 + m_i^2$ (where p_i being the momentum of the i^{th} quark) and ε and ε', the polarization vectors of h and h' vector mesons in the above equation, we can express Eq.(4.2.48) as,

$$M_{fi} = \sqrt{\frac{2}{3}}(2\pi)^8[TR]\frac{N_h N_{h'} N_{h''}}{(2\pi)^3}\chi,$$
$$\chi = \int d^4q \frac{D_h(\widehat{q})D_{h'}(\widehat{q'})D_{h''}(\widehat{q''})\phi_h(\widehat{q})\phi_{h'}(\widehat{q'})\phi_{h''}(\widehat{q''})}{\Delta_1\Delta_2\Delta_3},$$
$$[TR] = Tr[i\gamma\varepsilon(-i\gamma.p_1+m)i\gamma.\varepsilon'(-i\gamma.p_3+m)\gamma_5(i\gamma.p_2+m)], \quad (4.2.54)$$

where $[TR]$ is the trace over the product of the gamma matrices coming from the hadron-quark vertex functions for the three mesons and the internal quark propagators, and can be expressible as: $[TR] = i4m\epsilon_{\mu\nu\lambda\alpha}\varepsilon_\mu\varepsilon'_\nu P_\lambda Q_\alpha$, ($2Q = P' - P''$ being the difference of momenta of the two outgoing mesons), while χ is the four-dimensional integral over d^4q given above. Thus, one can obtain the invariant amplitude for the process as[50],

$$M_{fi} = i4\sqrt{\frac{2}{3}}(2\pi)^5 m N_h N_{h'} N_{h''}\epsilon_{\mu\nu\lambda\alpha}\varepsilon_\mu\varepsilon'_\nu P_\lambda Q_\alpha\chi. \quad (4.2.55)$$

In the expression for M_{fi} above, $N_{h'}$ and $N_{h''}$ are the 4D BS normalizers for vector and pseudoscalar mesons respectively in the final state, while N_h is the BS normalizer for vector meson in the initial state. These BS normalizers are evaluated from Eq.(2.4.63) and Eq.(2.4.67). The numerical values of BS normalizers for $\omega(1420)$, $\rho(1450)$, $\rho(770), \omega(782)$ and $\pi(140)$ mesons so obtained are listed in the section on Numerical Calculations.

4.2.2 Calculation of the four dimensional integral, χ

To calculate the integral, χ, in Eq.(4.2.54), which involves integration over $d^4q = d^3\widehat{q}Md\sigma$, we first express internal momenta q' (of hadron h') and q'' (of hadron h'')) in terms of q (of hadron h) and then try to express the integrand in terms of the variables, $\widehat{q}$ and σ. From the relations between the momenta in Eq.(4.2.43-4.2.46), we can express the momentum of the third quark, $p_3 = -\frac{1}{2}P' + \frac{1}{2}P'' + q$, which can in turn be written as

$$p_3^2 = -\frac{M^2}{4} + \widehat{q}^2 - M^2\sigma^2 - M''^2\sigma'' + M'^2\sigma' \tag{4.2.56}$$

eventually giving rise to, $\Delta_3 = m^2 + p_3^2$ as,

$$\Delta_3 = -\frac{M^2}{4} - M^2\sigma^2 - M''^2\sigma'' + M'^2\sigma' + \omega^2, \tag{4.2.57}$$

where $\omega^2 = \widehat{q}^2 + m^2$. Since $p_1^2 = \frac{P^2}{4} + P.q + q^2 = {p_1'}^2 = \frac{P'^2}{4} + P'.q' + q'^2$, one can obtain

$$-M^2(\sigma + \frac{1}{2})^2 + \widehat{q}^2 = -M'^2(\sigma' + \frac{1}{2})^2 + \widehat{q'}^2, \tag{4.2.58}$$

from which one can express the square of the transverse momentum of hadron h' as,

$$\widehat{q'}^2 = \widehat{q}^2 - M^2(\sigma + \frac{1}{2})^2 + M'^2(\sigma' + \frac{1}{2})^2. \tag{4.2.59}$$

Also since, $p_2^2 = \frac{P^2}{4} - P.q + q^2 = p_2''^2 = \frac{P''^2}{4} - P''.q'' + q''^2$, one can obtain

$$-M^2(\sigma - \frac{1}{2})^2 + \widehat{q}^2 = -M''^2(\sigma'' - \frac{1}{2})^2 + \widehat{q''}^2, \tag{4.2.60}$$

and thus the square of the transverse momentum of hadron h'' is given as,

$$\widehat{q''}^2 = \widehat{q}^2 - M^2(\sigma - \frac{1}{2})^2 + M''^2(\sigma'' - \frac{1}{2})^2. \tag{4.2.61}$$

As we see from Eq.(4.2.57), Eq.(4.2.59) and Eq.(4.2.61), each of $\Delta_3, \widehat{q'}^2$ and $\widehat{q''}^2$ are not only functions of the integration variables σ and $\widehat{q}$, but also functions of dependent variables σ' and σ''. However, from Eq.(4.2.46) one can obtain $P.q' = \frac{P.P"}{2} + P.q$. In the rest frame of the initial hadron $P = (0, iM)$, M being its rest mass, the momenta of hadrons, h', h'' in final state are: $P' = (\overrightarrow{P'}, iE')$ and $P'' = (\overrightarrow{P''}, iE'')$ respectively. Since $q' = (\widehat{q'}, iM'\sigma')$, M' being the rest mass of one of hadrons h', $P.q' = -MM'\sigma'$,

$\frac{P.P''}{2} = -\frac{ME''}{2}$, where E'' is the energy of hadron h'' (ie. the pion) in the final state, and $P.q = -M^2\sigma$. Hence,

$$\sigma' = \frac{M}{M'}\sigma + \frac{E''}{2M'}. \tag{4.2.62}$$

Similarly, from Eq.(4.2.46) one can also obtain $P.q'' = -\frac{P.P'}{2} + P.q$. And since $q'' = (\widehat{q''}, iM'')$, M" being the rest mass of the pion, we get $P.q'' = -MM''\sigma''$, and $-\frac{P.P'}{2} = \frac{ME'}{2}$, where E' is the energy of the h' meson. Thus,

$$\sigma'' = \frac{M}{M''}\sigma - \frac{E'}{2M''}. \tag{4.2.63}$$

Now, substituting the above equations for σ' and σ'' into Eq.(4.2.57), Eq.(4.2.59) and Eq.(4.2.61), one can express all $\Delta_3, \widehat{q'}$ and $\widehat{q''}$ in terms of only the integration variables σ and $\widehat{q}$(or ω). Moreover, E' and E'' are determined from conservation of energy and which are given by $E' = \frac{M^2+M'^2-M''^2}{2M}$ and $E'' = \frac{M^2-M'^2+M''^2}{2M}$. This allows us to express the time-like momenta σ' and σ'' of the two emitted hadrons in terms of the time-like momentum, σ of the initial meson as,

$$\begin{aligned} \sigma' &= \frac{M}{M'}\sigma + \frac{M^2 - M'^2 + M''^2}{4MM'}, \\ \sigma'' &= \frac{M}{M''}\sigma - \frac{M^2 + M'^2 - M''^2}{4M''M}. \end{aligned} \tag{4.2.64}$$

Thus from Eq.(4.2.59) and Eq.(4.2.61), we note that the squares of the transverse components of internal momenta of the two emitted hadrons, h', h'' involves the time-like momenta of the initial hadron, h as:

$$\begin{aligned} \widehat{q'}^2 &= \widehat{q}^2 - M^2(\sigma + \frac{1}{2})^2 + M'^2[\frac{M}{M'}\sigma + \frac{M^2 - M'^2 + M''^2}{4MM'} + \frac{1}{2}]^2, \\ \widehat{q''}^2 &= \widehat{q}^2 - M^2(\sigma - \frac{1}{2})^2 + M''^2[\frac{M}{M''}\sigma - \frac{M^2 + M'^2 - M''^2}{4MM''} - \frac{1}{2}]^2. \end{aligned} \tag{4.2.65}$$

Hence the two 3D gaussian wave functions, $\phi(\widehat{q'}) = e^{-\frac{\widehat{q'}^2}{2\beta'^2}}$ and $\phi(\widehat{q''}) = e^{-\frac{\widehat{q''}^2}{2\beta''^2}}$ (in Eq.(4.2.51)) in final state corresponding to two emitted hadrons will involve the time-component of momentum of the initial hadron,σ. Due to the fact that there are three hadron-quark vertex functions entering the triangle quark diagram in the process, $h \to h' + h''$ (with two gaussian functions corresponding to two hadrons in final state), the calculation of loop integral χ is more complex than the corresponding problem encountered in calculation of radiative decays of vector mesons through the process $h \to h'\gamma$ (where only one gaussian function $\phi(\widehat{q}')$ corresponding to one hadron in final state was involved)[(46)] dealt recently.

We now try to solve this problem in the context of strong decays of hadrons through the process, $h \to h' + h''$. Now the 4D integral, χ in Eq.(4.2.54) involves the denominator functions, $D_h(\widehat{q}), D_{h'}(\widehat{q}')$ and $D_{h''}(\widehat{q}'')$. Though $D_h(\widehat{q})$ is simple to evaluate by direct contour integration over the complex σ plane by noting the positions of poles through $\Delta_{1,2} = 0$, and is given by the first two equations of Eq.(4.2.69) below, and is thus expressed as:

$$\frac{1}{D_h(\widehat{q})} = \frac{1}{2\pi i}\int_{-\infty}^{\infty}\frac{Md\sigma}{\Delta_1\Delta_2} = [\omega(4\omega^2 - M^2]^{-1}, \tag{4.2.66}$$

the evaluation of $D_{h'}(\widehat{q}')$ and $D_{h''}(\widehat{q}'')$ is not simple, since their evaluations involve integrations over $d\sigma'$ and $d\sigma''$ and also over the poles positions of Δ_3, which is quite an involved expression given in Eq.(4.2.69) below. But from Eq.(4.2.64), we can obtain $M'd\sigma' = Md\sigma$, and $M''d\sigma'' = Md\sigma$. Now we have to get expressions of denominator functions $D_{h'}(\widehat{q}')$ and $D_{h''}(\widehat{q}'')$ in terms of the integration variables $\widehat{q}$ and σ of the initial meson. They are expressed as,

$$\begin{aligned}\frac{1}{D_{h'}(\widehat{q}')} &= \frac{1}{2\pi i}\int_{-\infty}^{\infty}\frac{M'd\sigma'}{\Delta_1\Delta_3} = \frac{1}{2\pi i}\int_{-\infty}^{\infty}\frac{Md\sigma}{\Delta_1\Delta_3},\\ \frac{1}{D_{h''}(\widehat{q}'')} &= \frac{1}{2\pi i}\int_{-\infty}^{\infty}\frac{M''d\sigma''}{\Delta_2\Delta_3} = \frac{1}{2\pi i}\int_{-\infty}^{\infty}\frac{Md\sigma}{\Delta_2\Delta_3}.\end{aligned} \tag{4.2.67}$$

To calculate $D_{h'}(\widehat{q}')$ and $D_{h''}(\widehat{q}'')$, we first express the quantity $\Delta_i = m_i^2 + p_i^2$, (corresponding to ith quark, with $i = 1, 2, 3$) in terms of the integration variable σ as,

$$
\begin{aligned}
&\Delta_{1,2} = -M^2(\sigma \pm \frac{1}{2})^2 + \omega^2, \\
&\Delta_3 = -\frac{M^2(M - M' - M'') + (M' - M'')^2(M' + M'')}{4M} \\
&+M(M' - M'')\sigma - M^2\sigma^2 + \omega^2.
\end{aligned} \tag{4.2.68}
$$

Then, to calculate these integrals over $d\sigma$, we note the positions of poles of the propagators in the complex σ-plane as:

$$
\begin{aligned}
&\Delta_1 = 0 \Rightarrow \sigma^{\pm} = \pm\frac{\omega}{M} - \frac{1}{2} \mp i\epsilon, \\
&\Delta_2 = 0 \Rightarrow \sigma^{\pm} = \pm\frac{\omega}{M} + \frac{1}{2} \mp i\epsilon, \\
&\Delta_3 = 0 \Rightarrow \sigma^{\pm} = \frac{4M^2(M' - M'') - \sqrt{f}}{8M^3} \mp i\epsilon, \\
&f = 16M^3 \times \\
&[-M^3 + (M - M' - M'')(M' - M'')^2 + M^2(M' + M'') + 4M\omega^2]
\end{aligned} \tag{4.2.69}
$$

so that the analytic expressions for both denominator functions, $D_{h'}(\widehat{q'})$ and $D_{h''}(\widehat{q"})$ can be worked out and are expressible in terms of ω (which involves the 3-D integration variable $\widehat{q}$). These two expressions are quite lengthy and we do not present their full forms here. Moreover, we can also express the corresponding 3D wave functions of hadrons in final state, $\phi(\widehat{q'})$ and $\phi(\widehat{q"})$ in terms of the integration variables σ and $\widehat{q}$ corresponding to hadron in initial state through Eq.(4.2.51). Thus, the integrand of 4D integral χ in Eq.(4.2.54) is fully expressible in terms of time-like variable σ and 3D variable, $\widehat{q}$. Integration over $d\sigma$ is first done analytically followed by numerical integration over the 3D variable $d^3\widehat{q}$ using Mathematica, giving us numerical value for the 4-dimensional integral, χ appearing in Eq.(4.2.54) which will be employed for decay width calculation for various processes in the next section.

4.2.3 Calculation of the decay width

To calculate the decay width, we need the form of the invariant amplitude M_{fi}, which is given in Eq.(4.2.55). Now, in the rest frame of the initial hadron, $\overrightarrow{P} = 0$ (i.e. $\overrightarrow{P'} = -\overrightarrow{P"}$), the total decay rate can be worked out as:

$$\Gamma = \frac{|\overrightarrow{P'}|}{8\pi M^2}\overline{|M_{fi}|}^2, \tag{4.2.70}$$

where the spin averaged invariant amplitude squared, $\overline{|M_{fi}|}^2 = \frac{1}{3}\sum_{s_1=1}^{3}\sum_{s_2=1}^{3}|M_{fi}|^2$ can be expressed as,

$$\overline{|M_{fi}|}^2 = \frac{64(2\pi)^{10}}{81}m^2M^2N_h^2N_{h'}^2N_{h''}^2|\overrightarrow{P'}|^2|\chi|^2. \tag{4.2.71}$$

Thus, the total decay rate is equal to

$$\Gamma = \frac{16(2\pi)^9m^2N_h^2N_{h'}^2N_{h''}^2}{81}|\overrightarrow{P'}|^3|\chi|^2, \tag{4.2.72}$$

where $|\overrightarrow{P'}|$ is given by

$$|\overrightarrow{P'}| = \frac{M}{2}\sqrt{1+\frac{M'^4}{M^4}+\frac{M"^4}{M^4}-2\frac{M'^2}{M^2}-2\frac{M"^2}{M^2}-2\frac{M'^2M"^2}{M^4}}. \tag{4.2.73}$$

The decay widths for the processes studied are given in the next section.

4.2.4 Numerical calculation

The input parameters employed in the calculation are: $C_0 = .29, \Lambda = .200\text{GeV}$, $\omega_0 = 0.158\text{GeV}$, $m_{u,d} = 0.265\text{GeV}$[19]. In the process, $h \to h' + h''$ studied here, the mesons in initial state are: $\omega(1420)$ and $\rho(1450)$, with their experimental masses

1.420GeV and 1.450GeV respectively. The experimental meson masses appearing in the final states in the above process are taken as: $M_\pi = .140$GeV, $M_\rho = .770$GeV and $M_\omega = .782$GeV. The numerical values of BS Normalizers for mesons in the initial states are calculated to be: $N_{\omega(1420)} = .556GeV^{-3}$ and $N_{\rho(1450)} = .525GeV^{-3}$, while their values for those in the final state are: $N_\pi = .599GeV^{-3}$, $N_\rho = .359GeV^{-3}$, and $N_\omega = .347GeV^{-3}$. The calculated values of the decay widths are given below[50] along with the corresponding central values of data in brackets as:

$$\Gamma(\omega(1420) \rightarrow \rho + \pi) = 141\text{MeV}(\text{Expt.} = (125.8 - 174.7)\text{MeV}^{(47)})$$
$$\Gamma(\rho(1450) \rightarrow \omega + \pi^0) = 98.6\text{MeV}(\text{Expt.} = 84\text{MeV}^{(47)}). \qquad (4.2.74)$$

4.2.5 Discussions

In the second section, we have employed Bethe-Salpeter framework under Covariant Instantaneous Ansatz (CIA) to calculate the strong decay widths for the processes: $\omega(1420) \rightarrow \rho + \pi$ and $\rho(1450) \rightarrow \omega + \pi$ using Feynman diagrams in leading order which happen to be the triangle quark-loop diagrams. These triangle loop diagrams are more complex than the two-quark loop diagrams which are involved in processes like $V \rightarrow e^+ + e^-$, or $P \rightarrow l + \overline{\nu_l}$ and are represent sensitive probes of the internal dynamics of $q\overline{q}$ hadron. In the first section, we were involved in solving the problem $h \rightarrow h' + \gamma$, which also proceeds through triangle loop diagram.

The main motivation for these two works is to test the applicability of our BSE formalism under CIA to processes which proceed through triangle quark-loop diagrams, and in the process to resolve the problems involved in the calculations of such diagrams in BSE under CIA, which give rise to extremely complex 4D loop integrals (as pointed out earlier in ref.[17]) due to appearance of time-like momentum components in gaussian factors associated with the vertex functions of the participating hadrons. We made use of similar techniques employed in resolving complexities in amplitudes for such triangle loop diagrams in BSE under CIA in $h \to h' + \gamma$ to study strong decays of radially excited vector mesons, $h \to h'h''$ in the second section, which is a more complicated problem due to presence of two hadrons in the final state as explained below.

Regarding the relative complexities of the calculations involved in (i) $h \to h' + h''$, and (ii) $h \to h' + \gamma$, it is to noted that the invariant amplitude M_{fi} in the former case is more complex than that in the latter case due to presence of three hadron-quark vertices operative at the three corners of quark-loop, in contrast to only two hadron-quark vertices operative in $h \to h'\gamma$. This in turn makes the 4D loop integral, χ in Eq.(4.2.54) in present calculation on $h \to h' + h''$ more complex than the corresponding 4D loop integral in $h \to h'\gamma$ due to presence of an extra $[D(\widehat{q})\phi(\widehat{q})]$ in its integrand corresponding to an extra hadron h'' in the final state.

Thus, in this more involved process, $h \to h' + h''$, due to three hadron-quark vertex functions operative in the diagram, there are three gaussian wave functions $\phi_h(\widehat{q})$, $\phi_{h'}(\widehat{q'})$ and $\phi_{h"}(\widehat{q}")$ in the 4D loop integral χ (instead of only two gaussian functions in the corresponding 4D loop integral in $h \to h' + \gamma$). We further see the mixing of time component of momentum σ of initial vector meson in the squares of the effective 3D vectors and hence in the Gaussian wave functions for both vector meson, $Exp[-\widehat{q}'^2/2\beta'^2]$ as well as the pseudoscalar meson $Exp[-\widehat{q}''^2/2\beta''^2]$ (due to Eq.(4.2.65) in the final state of the process $h \to h' + h''$ in contrast to $h \to h' + \gamma$ where there is mixing of time component of initial meson in the Gaussian wave function of a single pseudoscalar meson in the final state. Due to this, the calculation of the loop integral, χ in $h \to h' + h''$ is more complex than the calculation of the loop integral in $h \to h' + \gamma$.

However, though the expression for trace over the gamma matrices, $[TR]$ in both processes looks similar, the $[TR]$ in $h \to h'h''$ involves polarization vector of both the vector mesons h and h' involved in the process, in contrast to $[TR]$ in $h \to h'\gamma$, which involves polarization vectors of a vector meson h and γ. Due to this, the decay width expression (which involves calculation of $|\overline{M_{fi}}|^2$) is again more involved in $h \to h' + h''$ than in $h \to h' + \gamma$. In the second section we have shown explicitly how to handle this problem and calculate meaningful results for $h \to h + h$. The calculated values of the decay widths for the above processes are given below[50] along with the corresponding central values of data in brackets as:

$$\begin{aligned}
&\Gamma(\omega(1420) \to \rho + \pi) = 141\text{MeV}(\text{Expt.} = (125.8 - 174.7)\text{MeV}^{(47)}) \\
&\Gamma(\rho(1450) \to \omega + \pi^0) = 98.6\text{MeV}(\text{Expt.} = 84\text{MeV}^{(47)}).
\end{aligned} \tag{4.2.75}$$

We present in Table 4.1, the results of our model along with those of other models[43−46] and experimental data [47].

	BSE-CIA	NJL[43]	$^3P_0$ Decay[44]	Chiral[45]	[46]	Expt.[47]
$\omega(1420) \to \rho + \pi$	141	225	328	422	820	125.8-174.7
$\rho(1450) \to \omega + \pi$	98.6	75	122	165	280	84

Table 4.1: Values of Decay widths Γ (in MeV) in various models along with central values of experimental data (in last column) for processes, $\omega(1420) \to \rho + \pi$ and $\rho(1450) \to \omega + \pi$

The wide range of variation of experimental data on decay widths for $\omega(1420)$[47] is to be noted. We further see that different models also seem to have a wide range of variations in values of decay widths for both these processes. Though our results of BSE under CIA (in 1st column of Table 1) are in rough agreement with experiment, as regards comparison with other models is concerned, there is some resemblance of our results particularly with regard to $\rho(1450)$ decay width with the corresponding results of NJL model [43] and $^3P_0$ decay model[44] . However our results of $\omega(1420)$ decay width is small in comparison to the results in both these models. Also, our results are much lower in comparison to results of Chiral model[45] ,as well as the results in[46] whose values are on the higher side. The large variations in the results of various models as well as experimental data signifies that there is still lack of clear understanding with regards the decays of these mesons and requires further work.

Chapter 5

Summary and conclusion

This thesis is organized as follows: chapter 1 deals with a review of QCD gauge theory. Derivation of Bethe-Salpeter equation (BSE) is done in chapter 2. Application of BSE to some high and low energy processes is done in chapter 3 and 4. QCD is regarded as the non Abelian gauge theory for strong interaction dynamics. The fundamental degrees of freedom are quarks and gluons which interact through color charge. Color is to QCD what electric charge is to QED. The force between two quarks is mediated by the exchange of 8 colored gluons unlike in QED where the force between two electrons is mediated by exchange of a photon. However due to the non Abelian nature of QCD, the gluons can also self couple with one another leading to 3 gluons and 4 gluons vertices, unlike in Abelian QED where the photons do not self interact. This self coupling of gluons in QCD leads to interesting properties of asymptotic freedom(QCD coupling constant becoming small at large momentum transfer, Q^2) and confinement(QCD coupling constant becoming large at small momentum transfer, Q^2.) This behavior of QCD coupling constant $\alpha_s(Q^2)$ is in complete contrast to the behavior of QED coupling constant α which is small at low Q^2 and large at high Q^2. Thus in chapter 1, as a mathematical preliminary we first review QCD gauge theory.

The full QCD Lagrangian is first derived using the principle of local gauge invariance on free Dirac Lagrangian. We then study the fundamental one loop diagrams in QCD corresponding to the processes of self energy, vacuum polarization and vertex corrections. These graphs containing loops lead to divergent integrals. The renormalization of these integrals is done using dimensional regularization. The running coupling constant $\alpha_s(Q^2)$ is then derived. Due to small values of $\alpha_s(Q^2)$ at high energies, the QCD perturbation theory is only applicable to high energy processes. However in the confinement region(low Q^2), $\alpha_s(Q^2)$ is large and we need non perturbative methods. One of the popular non perturbative approach is the one employing Bethe-Salpeter Equation(BSE) which is firmly rooted in field theory. The detailed derivation of BSE is presented in chapter 2. We also presented here the derivation of 4D hadron-quark vertex function Γ in BSE under Covariant Instantaneous Ansatz(CIA). This CIA is a Lorentz invariant generalization of Instantaneous Approximation(IA). This 4D hadron-quark vertex function $\Gamma(\hat{q})$ provides a fully Lorentz invariant basis for evaluation of various transition amplitudes through quark-loop diagrams. The calculation of BS normalizers N_P and N_V for pseudoscalar and vector mesons is also presented in detail in this chapter. In chapter 3 we studied the high energy production process $e^+ + e^- \to J/\psi + \eta_c$ at center of mass energy $\sqrt{s} = 10.6 GeV$ which has recently been studied at B-factories and whose measurements were done be Babar(24) and Belle(25,26) groups. We studied this process in BSE framework under CIA to calculate the cross section whose value we worked out as $\sigma(e^+ + e^- \to J/\psi + \eta_c) = 21.75 fb$(33) which is in broad agreement with Babar data $\sigma(e^+ + e^- \to J/\psi + \eta_c) = (17.6 \pm 2.8 \pm 2.1) fb$(24) and Belle data $\sigma(e^+ + e^- \to J/\psi + \eta_c) = (25.6 \pm 2.8 \pm 3.4) fb$(25,26). In chapter 4 we employed BSE under CIA to calculate low energy processes: (i)the radiative decay widths of equal mass vector mesons (ρ, ω) through the process $h \to h'\gamma$ and (ii) strong decays of radially excited vector mesons $\rho(1450)$ and $\omega(1420)$ through the process $h \to h' + h"$ using leading order Feynman diagrams. We have calculated the radiative decay widths for the processes: $\rho^{\pm} \to \gamma\pi^{\pm}$, $\rho^0 \to \gamma\pi^0$ and $\omega \to \gamma\pi^0$. The motivation for this work was our intention to resolve the problems involved in the calculations of triangle quark loop diagrams which appear in processes such as radiative meson decays, strong decays of hadrons etc. in BSE under CIA, which gives rise to extremely complex 4D loop integrals due to appearance of time like momentum components in gaussian factors associated with the vertex functions of the participating hadrons. In these processes involving quark triangle loop diagrams, it is to be noted that the square of the effective 3D vector for pseudoscalar meson $\widehat{q'}^2$, involves not only the square of the effective 3D vector for vector meson, $\widehat{q}^2$, but also the mixing from the time like momentum components σ of the vector meson, and hence leading to the appearance of time-like (σ) momentum components in the gaussian factors in the 3D wave function, $\phi_P(\widehat{q'})$ associated with the vertex function $\Gamma^P(\widehat{q'})$ of pseudoscalar meson. This is the root cause of complexity in the calculations of transition amplitudes for such processes involving triangle loop diagrams. In this work we have tried to show how to handle such problems and calculate meaningful results. Our results for decay widths in Eq.(4.1.41) can also be compared with results of some other calculations [40,41,42]. In a calculation under BSE framework [40], the decay widths calculated were: $\Gamma(\rho^{\pm} \to \gamma\pi^{\pm}) = .38 \times 10^{-4}$GeV, $\Gamma(\rho^0 \to \gamma\pi^0) = .38 \times 10^{-4}$GeV and $\Gamma(\omega \to \gamma\pi^0) = 3.35 \times 10^{-4}$GeV. In a recent calculation using Salpeter Equation based model [41,42], the results of radiative decay widths were: $\Gamma(\rho^{\pm} \to \gamma\pi^{\pm}) = .35 \times 10^{-4}$GeV, $\Gamma(\rho^0 \to \gamma\pi^0) = .35 \times 10^{-4}$GeV, and $\Gamma(\omega \to \gamma\pi^0) = 3.15 \times 10^{-4}$GeV. In another calculation using Salpeter equation by the same group but using a different form of confining potential(41,42), the results of decay widths were: $\Gamma(\rho^{\pm} \to \gamma\pi^{\pm}) = .21 \times 10^{-4}$GeV, $\Gamma(\rho^0 \to \gamma\pi^0) = .21 \times 10^{-4}$GeV and $\Gamma(\omega \to \gamma\pi^0) = 1.85 \times 10^{-4}$GeV. These results of other models are in broad agreement with our results.

In the third problem we have considered strong decays of radially excited 2s vector mesons $\rho(1450)$ and $\omega(1420)$ through the processes $\omega(1420) \to \rho\pi$ and $\rho(1450) \to \omega + \pi^0$ using Feynman diagrams in lowest order. Using the techniques developed in the above problem $h \to h' + \gamma$, the calculated values of the decay widths are given below(50) along with the corresponding central values of data in brackets as:

$$\begin{aligned}
&\Gamma(\omega(1420) \to \rho + \pi) = 141\text{MeV}(\text{Expt.} = (125.8 - 174.7)\text{MeV}^{(47)}) \\
&\Gamma(\rho(1450) \to \omega + \pi^0) = 98.6\text{MeV}(\text{Expt.} = 84\text{MeV}^{(47)}). \qquad (5.0.1)
\end{aligned}$$

The results of our model along with those of other models and data are given in Table 4.1 in chapter 4. The wide range of variations in results of various models and experimental data is to be noted. Our results are in rough agreement with experiment.

In the calculation $h \to h' + h$" we attempted, we were mainly motivated by the desire to address the problems associated with triangle loop diagrams in BSE under CIA in the context of strong decays of excited vector mesons. We wish to mention that in the present work, we employed only the most leading of the Dirac structures $i\gamma.\varepsilon$ and γ_5 in the hadron-quark vertex functions for vector and pseudoscalar mesons respectively. We do hope that our results can be further improved by including the Next-to-leading order (NLO) Dirac structures in accordance with the power counting rule developed in[21]. However, the techniques involved in these calculations for handling triangle loop diagrams in CIA, developed in this work can in turn be employed to calculations of many other processes.

With this successful application of CIA framework to radiative decays of equal mass vector meson, we now intend to generalize this framework to decays of unequal mass vector mesons (which involve unequal mass kinematics) and also the application of this framework to other processes involving quark-triangle diagrams.

The techniques involved in these calculations for handling triangle loop diagrams in CIA, developed in this work can in turn be employed to calculations of high energy production processes involving quark -triangle diagrams like double charmonium production in electron-positron collisions such as $e^- + e^+ \rightarrow J/\psi + \eta_c$. In chapter 3 this process was done employing heavy quark approximation which simplified the loop integrals considerably. We now intend to study this process (without using the heavy quark approximation) by making use of the techniques developed in this thesis for our next study.

In conclusion, BSE under CIA is one of powerful tool to investigate hadronic processes right from low energies to high energies the results of which are in reasonable agreement with data.

Finally, we hope this work leads to a deeper understanding of hadronic structures and their interactions.

Bibliography

[1] Murry Gell-Mann, Physics letters 8, 214(1964); Phys. Rev. 125(1962).

[2] George Zweig, Orgins of the quark model,CAL Tech Report, CALT-68-805(1980).

[3] K.G.Wilson, Rev.Mod.Phys. 55,583(1983).

[4] G.P.Lepage, hep-lat/0506036(2005).

[5] N. Brambilla et al., arXiv:hep-ph/0412158.

[6] W.Marciano, H.Pagles, Phys.Rep.36.137-276(1978).

[7] E.S.Abers, B.W.Lee,Phys.Rep.9,1-141(1973).

[8] Andreas S Kronfeld, Quantum chromodynamics with advanced computing,doi:10.1088/1742-6596/125/1/012067.

[9] Schwinger J (ed) 1958 Selected Papers in Quantum Electrodynamics (New York: Dover) ISBN 0-486-60444-6.

[10] Alcaraz J et al. (LEP) 2007 Precision electroweak measurements and constraints on the Standard Model (Preprint arXiv:0712.0929 [hep-ex]).

[11] Dixon L J 2007 Hard QCD processes at colliders, in 23rd International Symposium on Lepton-Photon Interactions at High Energy (Preprint arXiv:0712.3064 [hep-ph]).

[12] Greiner, Schramm, Stein, Quantum Chromodynamics, Second Edition, Springer.

[13] C.H.L.Smith, Ann.Phys.53,521(1969).

[14] E.E.Salpeter, Phys.Rev.87,328(1952).

[15] H.A.Bethe, E.E.Salpeter, Phys.Rev.84,1232(1951).

[16] N.Nakahishi, Prog,Theo.Phys.Suppl.43,1(1969).

[17] A. N. Mitra, B. M. Sodermark, Nucl. Phys. A **695**, 328 (2001) and references therein.

[18] S. Bhatnagar, D. S. Kulshreshtha, A. N. Mitra, Phys. Lett. B **263**, 485 (1991); A.N Mitra, S.Bhatnagar, intl.J.Mod.Phys. A7(1991).

[19] S. Bhatnagar, S-Y. Li, J. Phys. G **32**, 949 (2006).

[20] S.Bhatnagar, S-Y. Li, Intl. J. Mod. Phys. E 18, 1521(2009).

[21] S. Bhatnagar, S-Y.Li, J.Mahecha, Intl. J. Mod. Phys. E 20,1437 (2011); S.Bhatnagar,S-Y.Li, J.Mahecha, Proceedings of Intl. Symp. Nucl. Phys.(ISNP2009),Mumbai,India, Dec.8-12, 2009.

[22] J.Resag, C. R. Muenz, B. C. Metsch, H. R. Petry, Nucl. Phys. A **578**, 397 (1994).

[23] S. Bhatnagar, Intl. J. Mod. Phys. E **14**, 909 (2005).

[24] B.Aubert et al.[BABAR Collaboration], Phys. Rev. D **72**, 031101 (2005)[arxiv:hep-ex/0506062].

[25] K.Abe et al., et al.[BELLE Collaboration], Phys. Rev. Lett. **89**, 142001 (2002)[arxiv:hep-ex/0205104].

[26] K.Abe et al., et al.[BELLE Collaboration], Phys. Rev. D **70**, 071102 (2004)[arxiv:hep-ex/0407009].

[27] E.Braaten, J.Lee, Phys.Rev. **D67**, 054007 (2003).

[28] Y.J.Zhang, Y.J.Gao, K.T.Chao, Phys. Rev. Lett. **96**, 092001 (2006).

[29] B.Gong, J-X. Wang, arxiv:0712.4220[hep-ph].

[30] K.Hagiwara, E.Kou. and O.F.Qiao, to appear PLB, hep-ph/0305102.

[31] J.J Sakurai, Advanced Quantum Mechanics, Addison-Wesely Publishing Company.

[32] S.Bhatnagar and S.Y.Li, In the proceedings of 9th Workshop on Non-perturbative Quantum Chromodynamics, Paris, France, 4-8 Jun 2007, pp 12.

[33] E.Mengesha, S.Bhatnagar, Intl. J. Mod. Phys. E20, 2521 (2011), arxiv.org 1105.4944(hep-ph); E.Mengesha, S.Bhatnagar, Proceedings of DAE symposium in nuclear physics, vol.56, visakhapatnam, Dec.26-31, pg.872-873, India(http://www.symposium.org/proceedings/E65.pdf).

[34] G.Bodwin,E.Braaten,G. Lepage, Phys. Rev. D **51**, 1125 (1995); 55, 5855(E) (1997).

[35] K.Liu, Z.He, K.Chao, Phys. Lett. B **557**, 45 (2003).

[36] X-H Guo, H-W Ke, X-Q Li, X-H Wu, arxiv:0804.0949[hep-ph].

[37] D.Griffths, Introduction to Elementary Particles, Harper Row Publishers, N.Y. (1987). K. Nakamura et al.

[38] E.Mengesha, S.Bhatnagar, Intl. J. Mod. Phys. E21, 1250084 (2012).

[39] (Particle Data Group), J. Phys. G37, 075021 (2010).

[40] C.R.Munz et al., Phys. Rev. C 52, 2110 (1995).

[41] B.Metsch, hep-ph/0403118 (2004).

[42] M.Koll, R.Ricken, D.Merten, B.Metsch, H.Petry, Eur. Phys. J. A9, 73 (2000).

[43] E.A.Kuraev, M.K.Volkov, A.B.Arbuzov, Phys. Rev. C82, 068201 (2010).

[44] T.Barnes, F.E.Close, P.R.Page, E.S.Swanson Phys. Rev. D55, 4157 (1997).

[45] T.Gutsche, V.E.Lyubovitskij, M.C.Tichy, Phys. Rev. D79, 014036 (2009).

[46] N.N.Achasov, A.A.Kozhevnikov, Phys. Rev. D62, 117503 (2000).

[47] J. Beringer et al. (Particle Data Group), PR D86, 010001 (2012) (URL: http://pdg.lbl.gov).

[48] N.N.Singh, A.N.Mitra, Phys. Rev. D38, 1454 (1988).

[49] D.Arndt, C-R.Ji, hep-ph/9905360.

[50] E.Mengesha, S.Bhatnagar,, Int. J.Mod. Phys. E 22, 1350046 (2013).

LIST OF PUBLICATIONS

1. E.Mengesha, S.Bhatnagar, Intl. J.Mod. Phys. E20, 2521 (2011), arxiv.org 1105.4944(hep-ph)

2.E.Mengesha,S.Bhatnagar, Proceedings of DAE symposium in nuclear physics, vol.56, visakhapatnam , Dec.26-31, pg.872-873, India(http://www.symposium.org/proceedings /E65.pdf).

3.E.Mengesha, S.Bhatnagar, Intl. J.Mod. Phys. E21, 1250084 (2012).

4. E.Mengesha, S.Bhatnagar,, Int. J.Mod. Phys. E 22, 1350046 (2013).

5. Proceedings of the DAE Symp. on Nucl.Phys. 58 (2013).